

## INFORMATION TO USERS

This reproduction was made from a copy of a document sent to us for microfilming. While the most advanced technology has been used to photograph and reproduce this document, the quality of the reproduction is heavily dependent upon the quality of the material submitted.

The following explanation of techniques is provided to help clarify markings or notations which may appear on this reproduction.

1. The sign or "target" for pages apparently lacking from the document photographed is "Missing Page(s)". If it was possible to obtain the missing page(s) or section, they are spliced into the film along with adjacent pages. This may have necessitated cutting through an image and duplicating adjacent pages to assure complete continuity.
2. When an image on the film is obliterated with a round black mark, it is an indication of either blurred copy because of movement during exposure, duplicate copy, or copyrighted materials that should not have been filmed. For blurred pages, a good image of the page can be found in the adjacent frame. If copyrighted materials were deleted, a target note will appear listing the pages in the adjacent frame.
3. When a map, drawing or chart, etc., is part of the material being photographed, a definite method of "sectioning" the material has been followed. It is customary to begin filming at the upper left hand corner of a large sheet and to continue from left to right in equal sections with small overlaps. If necessary, sectioning is continued again—beginning below the first row and continuing on until complete.
4. For illustrations that cannot be satisfactorily reproduced by xerographic means, photographic prints can be purchased at additional cost and inserted into your xerographic copy. These prints are available upon request from the Dissertations Customer Services Department.
5. Some pages in any document may have indistinct print. In all cases the best available copy has been filmed.

**University  
Microfilms  
International**

300 N. Zeeb Road  
Ann Arbor, MI 48106



8323278

Elahi, Hamid

TRANSIENT STABILITY OF POWER SYSTEMS WITH NON-LINEAR LOAD  
MODELS USING INDIVIDUAL MACHINE ENERGY FUNCTIONS

*Iowa State University*

Ph.D.

1983

University  
Microfilms  
International 300 N. Zeeb Road, Ann Arbor, MI 48106



Transient stability of power systems with non-linear load  
models using individual machine energy functions

by

Hamid Elahi

A Dissertation Submitted to the  
Graduate Faculty in Partial Fulfillment of the  
Requirements for the Degree of

DOCTOR OF PHILOSOPHY

Department: Electrical Engineering

Major: Electrical Engineering (Power System)

Approved:

Signature was redacted for privacy.

In Charge of Major Work

Signature was redacted for privacy.

~~For the Major~~ Department

Signature was redacted for privacy.

For the Graduate College

Iowa State University

Ames, Iowa

1983

## TABLE OF CONTENTS

	Page
I. INTRODUCTION	1
II. REVIEW OF LITERATURE	7
A. Power System Load Representation	7
B. Direct Methods of Transient Stability Analysis in Power Systems	12
1. Early work on energy criterion for power system stability	13
2. Stability criterion for power systems using Lyapunov's direct method	14
3. Direct method of Lyapunov applied to the power system problem	16
4. Recent work on energy methods	17
5. Load representation in direct methods	21
C. Scope of the Work	22
III. MULTIMACHINE POWER SYSTEM REPRESENTATION	24
A. Classical Model with System Loads as Injected Currents	24
B. Procedure for Calculation of the Injected Load Currents	31

	Page
IV. TRANSIENT STABILITY ANALYSIS USING INDIVIDUAL ENERGY FUNCTIONS MODIFIED FOR NON-LINEAR LOADS	34
A. System Dynamic Equations in a Multimachine Power System	34
B. Transient Behavior of the Non-Linear Load Bus Angles	38
C. Individual Machine Transient Energy Function with Non-Linear Loads	39
D. Physical Interpretation of $V_i$	40
E. Transient Stability Assessment Criterion and Procedure	43
V. RESULTS	47
A. Test Networks	47
1. 4-generator, 11-bus system	47
2. 17-generator, 163-bus modified Iowa system	49
B. Computer Program	52
C. Model Accuracy	55
D. Stability Assessment	61
1. Stability assessment results	62
2. Effect of load model on transient stability	64
3. Two sources of error	68

	Page
VI. CONCLUSIONS	70
A. Conclusions Drawn Based on Proper Representation of Loads in Stability Studies	71
B. Conclusions Drawn Based on the Results of Chapter V	72
VII. REFERENCES	76
VIII. ACKNOWLEDGMENTS	80
IX. APPENDIX: COMPUTER PROGRAMS	81



## I. INTRODUCTION

Maintaining a reliable and uninterrupted electric service is among the primary objectives of the electric utility industry. To successfully meet this goal, power system planning engineers have devoted a good deal of their time and effort to study the transient stability of power systems under a variety of probable contingencies.

Transient stability studies are concerned with the stability characteristics of the electric power system under large and sudden disturbances. Following such disturbances, the terminal voltage, rotor angle, power and frequency of most synchronous machines will change, and the study lends itself to the determination and analysis of the transient behavior of these variables.

System equations, consisting of a set of non-linear differential equations coupled with a set of algebraic equations, e.g., the equations defining the network constraints, form the mathematical basis for the study. Conventionally, answers regarding the stability of the power system are postulated based on the time solution of the system equations, a tedious and time consuming task which is almost always carried out by digital computer simulations.

The most elementary representation of the multimachine interconnected power system, known as classical model, is

considered valid for the transient period in the order of one second or less. With this model, it is assumed that if the synchronous machines maintain synchronism for the first swing they will remain in synchronism thereafter. This is known in the power literature as "first swing" transient stability assessment.

Modern transient stability computer programs allow the use of detailed models for the turbine-generators and their controls. Transient stability studies are therefore usually carried out for transient periods of several seconds up to minutes following the disturbance initiating the transient. These elaborate, and costly, studies are now performed almost routinely by system planning engineers. The number of these studies has grown substantially, and the need for them has manifested itself in operating functions as well as in system planning functions.

The continuous growth of the power system both in complexity and size has resulted in a large and heavily interconnected system. Interconnections have mushroomed in the 1950s due to the following reasons: better economy of interchange, reduction in reserve power requirements, better reliability through support in emergencies, etc. While the presence of stronger ties between neighboring utility companies has made the power industry more dependent on the firm and emergency flow of power, building new transmission

facilities has become handicapped by such factors as high cost of capital, regulatory delays, right of way disputes, etc. In addition, recent fuel conservation policies have called for heavy use of energy sources other than costly oil and gas. Subsequently, the power network of North America has been operating under heavy loading of the transmission system and higher power transfers resulting in a more stressed and vulnerable transmission network.

For system planning studies, many more preliminary stability studies must be performed more frequently due to the added stress on the system, resulting in a net increase in the number of simulations. In addition, due to the growth of the power system, the computer simulation time has also grown rapidly. From the point of view of operation planning, where the system operators need to assess the robustness of the system for the short term forecasted operating conditions and outages, the application of the analytical approach is handicapped by the amount of time and effort necessary to prepare for detailed time solutions.

Direct methods of transient stability analysis offer alternative methods which are aimed at relaxing the technical and economical burdens associated with the analytical time solution approach. In addition, direct methods provide theoretical and physical interpretation of the transient behavior of the synchronous machines. Over

the last few decades, this fertile area of research has received a good deal of attention by the researchers (See the survey paper [1]). A brief chronological summary of the activities and developments in this area are also presented in Chapter II (Section B). The common features of the direct methods are:

1. The construction of a special function by which the stability characteristics of the system's post-disturbance equilibrium is directly examined.
2. An estimate of the region of stability (or Region of Attraction, ROA).

In this dissertation, the special function adopted is the individual machine energy function introduced by Vittal [2] and Michel et al. [3]. The key difference between the function developed in this work and the one in reference [2] is the treatment of the power system loads. In reference [2], loads were represented as constant shunt impedances and reported results were identical to those obtained by analytical time solution technique. This type of load representation is a major shortcoming of the above work.

The importance of the proper load representation in power system stability studies has long been recognized. Although it is generally acknowledged that the effect of

load representation is just as significant as the effect of the turbine-generator modeling on system stability, the former has received secondary attention. Load modeling, in general, is a difficult task basically because each electrical load exhibits a unique behavior depending on the time of the day, weather, human use patterns and most importantly the load composition.

Historically, constant shunt impedance representation of the load has been adopted for the real and reactive components of the load during the transient period [4-5]. Researchers studying the direct methods of stability analysis have also adopted the constant impedance model of the load. This linear representation of the load was part of the so-called classical model of the power system which was suited to simulation of the power system of the day (i.e., little interconnection, generation near the load, etc.) and the equipment of the day (i.e., slow excitation, etc.). This model gave adequate answers for first swing transient stability studies. However, in today's highly interconnected power system and in the presence of the highly sophisticated control devices (e.g., fast exciters, etc.) improvements must be made consistently to represent the components of the system more realistically. This dissertation is an attempt to address this issue in regard

to one of the most important components of the power system, namely the loads.

In this dissertation, non-linear voltage dependent loads are included as a modification to the classical model of the power system. The effect of the newly introduced load models now appear as injected currents at the internal nodes of the generators. Following the reduced admittance matrix formulation, a modified individual machine energy function has been derived to accommodate the new non-linear load representation.

Finally, using two test systems, a number of cases have been studied and results have been analyzed. It is hoped that this modified approach and the results presented in this dissertation contribute to the understanding of the effect of load representation in the study of first swing transient stability analysis using direct methods.

## II. REVIEW OF LITERATURE

### A. Power System Load Representation

In studying the dynamic behavior of power systems, much attention is devoted to the development and incorporation of correct and adequate representation of each component within the system. However, improvements regarding the accuracy of electrical load representation has received less attention compared to that given to those components of the power system such as generators and exciters. Lately this situation has changed and more attention has been focused on the representation of the loads in transient stability studies [6-13].

It has long been recognized that the transient behavior of the electrical load is a function of both frequency and voltage. Investigation of the frequency dependence of the load has revealed that the variation of active load with frequency has a direct effect on system damping, while the opposite is true for the variation of the reactive component of load [13]. In general, determination of load-frequency characteristics is a difficult task because of the difficulty in obtaining field measurements. Most transient stability programs have provisions to include frequency dependent load models but it is common to ignore the

frequency sensitivity of the loads, specially when voltage-MVA relationships are accounted for.

Comparatively more work has been done to investigate the effects of transient voltage fluctuations on electrical loads [4-13]. These studies have either been conducted with the effects of frequency changes present or only to study the voltage-MVA relationships of the load. References [5-7] have emphasized the need for a correct representation of electrical loads by reporting load voltage tests performed on different systems. References [8-10] have focused on load model developments for different load types based on collected field tests. Although each study has taken a different approach in the development of the load models and in the interpretation of the results, the common conclusion is that more detailed load models not only improve the design criterion but also exhibit significant effects on transient stability study results.

The inherent difficulties associated with determination of voltage-MVA characteristics of the loads are: non-homogeneity of the load composition in various areas of the power network, non-uniform patterns of voltage fluctuations under different disturbances, and discontinuities due to the operation of relays when big changes in system voltages take place, etc. Subsequently in every transient stability study attention must be paid to the choice of load models used for



the choice of load models used for the specific application of the study.

As far as the modeling of the loads for stability studies are concerned, the first model used was developed in the mid 30s. This model essentially assumes that the real and reactive components of the load vary with the square of the voltage. This linear model, known as constant impedance model, is still being widely used in stability studies. The argument in favor of the linear loads is that they are easily represented and do not require a simultaneous network solution for the period of application. On the other hand, their use has been strongly criticized because they do not reflect the true voltage-MVA relationship of the load. Depending upon the location of the disturbance, constant impedance loads could give unrealistically optimistic or pessimistic transient stability assessment.

To represent the voltage dependence of the loads, the following non-linear load models are commonly used: constant current and constant-MVA loads. Schematic representation of these models is shown in Figure 2.1. The constant current load is assumed to maintain the magnitude of the current drawn by the load to its pre-disturbance value. The constant-MVA model, on the other hand, maintains the real and reactive scheduled power constant (i.e., the same as the pre-disturbance values) regardless of how much voltage drops and how much current is drawn.

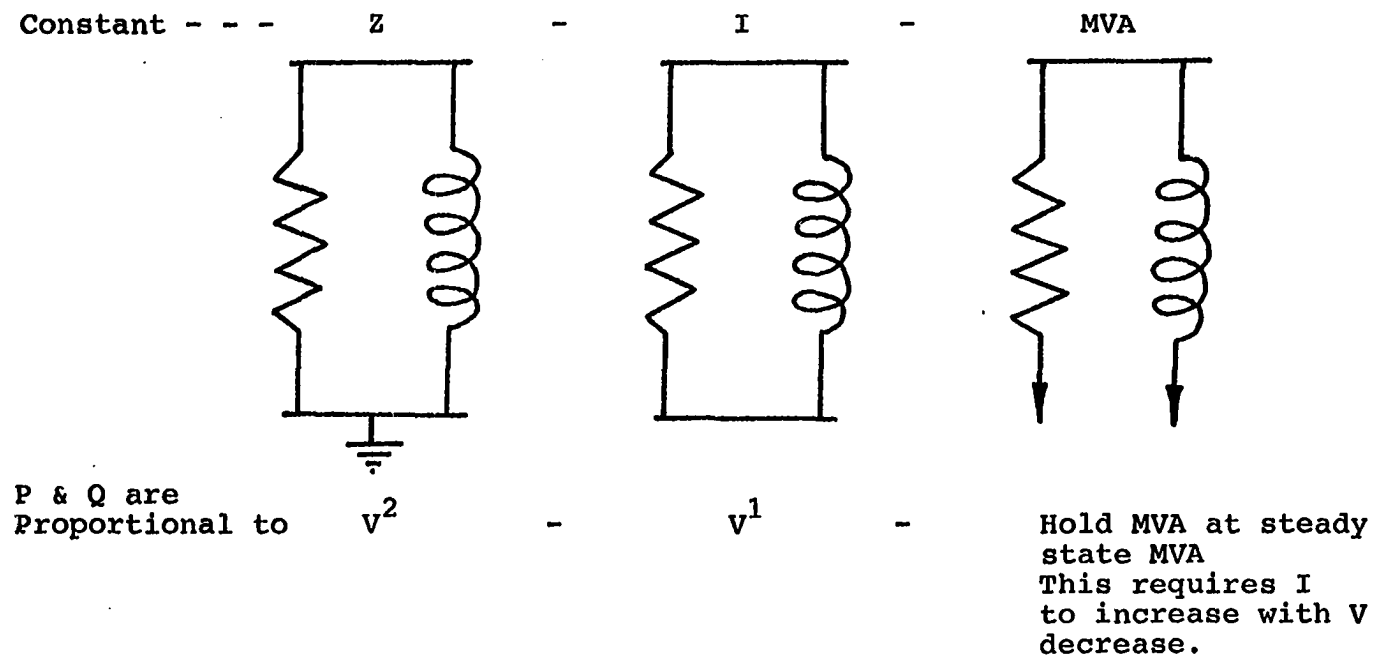


Figure 2.1. Load Modeled as constant  
(a) impedance (b) current (c) MVA

The constant impedance model of the load is suited for a class of loads known as static group. This group exhibits a constant near unity power factor (e.g., heating and lighting equipment). The constant-MVA model is a good model for another class of loads known as the rotating group. This group exhibits a constant-MVA and varying power factor (e.g., a mixture of synchronous or induction motors). Finally, the constant current loads are supposed to be made up of 50% constant impedance loads and 50% constant-MVA loads. It has been assumed that, in the aggregate, the transient response of electrical loads can be represented as some combination of constant impedance, constant current and constant-MVA loads.

Other efforts to model the load as a function of voltage could be summed up by two rather similar techniques. The first one expresses the load composition in terms of a quadratic polynomial of the form

$$\begin{aligned} P(v) &= K_0 + K_1 V + K_2 V^2 \\ Q(v) &= M_0 + M_1 V + M_2 V^2 \end{aligned} \tag{2.1}$$

where, at rated voltage, the values of  $K_0$ ,  $K_1$ ,  $K_2$  give  $P$  = scheduled real power, and the values of  $M_0$ ,  $M_1$ ,  $M_2$  give  $Q$  = scheduled reactive power.

Equation (2.1) represents the load composition in terms of the linear and non-linear load combination discussed earlier. The main criticism to this approach is due to the fact that the load polynomials do not pass through the origin in the voltage-MVA plane [10].

The other approach states that the voltage dependent loads could be modeled as

$$\begin{aligned}(P/P_o) &= (V/V_o)^n \\ (Q/Q_o) &= (V/V_o)^n\end{aligned}\tag{2.2}$$

where subscript  $_o$  indicates the pre-fault condition. In this technique, the exponent  $n$  signifies the voltage sensitivity of the load and its value is believed to vary somewhere between zero to three, according to the location and the nature of the load.

#### B. Direct Methods of Transient Stability Analysis in Power Systems

Direct methods of transient stability analysis in power systems are those methods in which transient stability assessment is made without obtaining time solution for the

system equations. The second (direct) method of Lyapunov provides the theoretical origin for these methods. For the system of dynamic equations and its post-disturbance stable equilibrium point (s.e.p.), a suitable Lyapunov function  $V$  is constructed. The region of stability around the post disturbance s.e.p. is then estimated. At the boundary of this region lies the critical value of  $V$ . This critical value can not be exceeded during the transient period if stability is to be maintained.

Many of the Lyapunov functions used are selected on the basis of energy considerations. They are called energy functions.

#### 1. Early work on energy criterion for power system stability

Based on the principle of conservation of energy, Gorev in 1930 [14], and Magnusson in 1947 [15] pioneered the research activities in the area of direct energy methods in power system. Using the lossless (zero transfer conductances) classical model of the power system, both authors have developed a criterion for transient stability. In 1958, Aylett [16] published his work

entitled "The energy-integral criterion of transient stability limits of power systems." He studied the nature of phase-plane trajectories of a multimachines system and arrived at the criterion for stability based on the comparison of the phase-plane trajectories with a critical trajectory which passes through the saddle-point and at which kinetic energy is equal to potential energy.

## 2. Stability criterion for power systems using Lyapunov's direct method

Several publications aimed at adopting the direct (second) method of Lyapunov to the problem of power systems transient stability followed the early work on energy methods.

The basis for using Lyapunov's direct method to obtain stability criterion for a multimachine power system is to express the post-disturbance autonomous system of power system dynamic equations as

$$\dot{\underline{x}} = \underline{f}(\underline{x}) \quad (2.3)$$

with  $\underline{f}(\underline{0}) = \underline{0}$  as the post-disturbance stable equilibrium state.

In the system described by (2.3), the elements of the state vector  $\underline{x}$  represent the rotor angles and the deviations in rotor speeds with respect to a synchronously rotating reference frame. Based on this system, a suitable scalar Lyapunov function  $V(\underline{x})$  is constructed. This function and its first derivative  $\dot{V}(\underline{x})$  must possess the required sign-definite properties. The criterion for stability is based on the construction of a region of stability (attraction) around the origin, or the post-disturbance stable equilibrium state. The value of  $V(\underline{x})$  at the boundary of this region is the critical value  $V_c(\underline{x})$ . To assess stability, a simple check is made. At the start of the post-disturbance period, the value of the Lyapunov function  $V(\underline{x})$  is compared to  $V_c(\underline{x})$ .

if  $V(\underline{x}) < V_c(\underline{x})$     system is stable.

if  $V(\underline{x}) > V_c(\underline{x})$     system is unstable.

For critical conditions, e.g., at critical clearing of a fault,  $V(\underline{x}) = V_c(\underline{x})$  .

Successful application of the direct method requires the following:

1. Construction of a valid Lyapunov function  $V(\underline{x})$
2. Estimate of the region of stability.

While there are no universal means available for the construction of the Lyapunov function, there are certain definiteness properties required for  $V(\underline{x})$  as well as its first derivative  $V'(\underline{x})$ .

3. Direct method of Lyapunov applied to the power system problem

In 1966, Gless [17] introduced Lyapunov's direct method in power system stability analysis. He used a single-machine infinite bus example and matched the results obtained by direct method to those obtained using equal area criterion. In the same year, El-Abiad and Nagappan [18] developed a Lyapunov function for a multimachine power system.

In order to construct a valid Lyapunov function for the power system problem, some of the early works had neglected the effect of transfer conductances [19]. This assumption often leads to conservative results and, as shown by Kitamura et al. [20], it could result into erroneous measure of critical clearing time in heavily loaded systems.



In reference [18], conservative estimate of the region of stability was obtained based on the assumption that the controlling unstable equilibrium point (u.e.p.) is the one closest to the stable equilibrium point (s.e.p.). In order to improve the estimate of the region of stability, Prabhakara and El-Abiad [21] and Gupta and El-Abiad [22] obtained better region of stability by accounting for the fault location in their choice for post-disturbance system's u.e.p.<sup>1</sup>

The survey papers by Fouad [1] and Ribbens-Pavella [23] offer an excellent overview of the research activities conducted on the development of stability criterion for power systems using Lypaunov's direct method.

#### 4. Recent work on energy methods

Within the last decade the following major contributions have resulted in the evolution of the direct energy methods as a practical tool for power systems transient stability analysis.

---

<sup>1</sup>Athay et al. [24,25] have also verified the fact that by appropriately accounting for fault location, the region of stability could be accurately assessed.

. Tavora and Smith [26], along with Lugtu and Fouad [27], have shown the significance of the Center of Inertia (COI) transformation from a synchronously rotating reference frame. This transformation removes that component of the transient energy responsible for the acceleration of the fictitious COI.

. In 1979, Athay and co-workers published their work entitled "A practical method for the direct analysis of transient stability" [24,25]. The major accomplishments as reported by the authors were:

1. By appropriately accounting for fault location (i.e., by determining the actual faulted trajectories) in the transient energy method, the stability of a multimachine system can be accurately assessed. The significance lies with the improved estimate of the region of stability, as mentioned earlier by [21,22].
2. Approximate techniques for incorporating the effects of transfer conductances on the power system transient behavior. Similiar approximations had also been proposed by Uyemura et al. [28].

3. Definition of the Potential Energy Boundary Surface (PEBS) which forms the basis for an important instability conjecture. This concept had been proposed by Kakimoto and co-workers in 1978 [29]. The critical clearing time obtained using the PEBS concept still resulted in conservative estimates for those cases where fault trajectory did not pass close to an u.e.p.

. In 1980, Fouad and co-workers [30,31], through extensive simulations on a practical power system, shed light on the physical aspect of the phenomenon of transient stability using direct energy methods. The authors have shown how to predict the correct mode of instability and how to assess the first swing transient stability using the value of the transient energy at the moment of last switching, the computed controlling u.e.p. and its energy. The authors have also pointed out that only the component of the transient kinetic energy associated with the gross motion of the critical generators is responsible for separation of the critical group from the rest of the system. The remaining portion of the transient kinetic energy could be identified with the inter-generator motion in each of the groups separating from one another. They also illustrated how instability could be determined by the

gross motion of the critical machines if more than one machine tend to lose synchronism. Finally, the authors have validated the concept of the controlling u.e.p. for a particular system trajectory.

. In 1982, Vittal [2] and Michel et al. [3] developed an individual machine energy function in order to identify the transient energy pulling a particular machine from the rest of the system. The energy function previously used by researchers was a system-wide energy function which masks the actual nature of the energy interchange in the system during the transient period. In this work, it was shown that under sustained fault conditions, the potential energy of the critical machine goes through a maximum which signifies the energy absorbing capacity (critical energy) of the critical machine. More importantly, for a given fault location and a given post-disturbance condition, this critical energy is fairly constant (flat) and its value is independent of the fault clearing time. Assessment of the first swing transient stability via individual machine energy functions was carried out for a series of simulations using three test networks. In all cases, the mode of instability was correctly predicted, even in very complex situations. The critical clearing time obtained matched the

results obtained by time solutions without any degree of conservatism.

## 5. Load representation in direct methods

All the works discussed in the previous section have consistently employed the classical model of the power system (i.e., generators represented by constant voltage behind transient reactances loads represented by constant shunt impedance, etc. See Chapter II of [32]). Although the classical model is generally considered satisfactory for the study of first swing transient stability, its greatest weakness lies in the representation of the loads. It is felt that improving the load model would substantially improve the confidence in first swing transient stability assessment results.

In the past, there have been some efforts to improve load representation when applying direct methods. Bergen and Hill [33] proposed a method to model frequency dependent loads by deriving a "topology preserving model" for the power network. Effect of each load was represented at its respective bus by a first order differential equation based on a load-frequency coefficient depicting the damping effect of the load. Athay and Sun [34] incorporated the static

non-linear load models in the expression for the system energy function. Network dependent variables were introduced in the energy function which does not allow the Kron reduction of the load buses. Pai et al. [35] modeled non-linear loads assuming constant ratio of internal bus voltages to load bus voltages corresponding to the pre-disturbance conditions. Musavi and Narasimhamurthi [36] assumed that the real part of the load is fixed while the reactive load is a function of the voltage at the load bus. Based on this assumption, the authors derived a "topological" energy function which brought the network dependent variables back in the picture.

Overall, incorporation of more realistic load models in the classical representation of the power system has either been accomplished at a substantial increase in the order of the system formulation or without an accurate account of the transient voltage fluctuations.

### C. Scope of the Work

This research work has concentrated on developing a technique to incorporate a more realistic model of the power system loads in the study of first swing transient stability analysis using individual machine energy functions.

Each electrical load has been represented as a combination of constant impedance, constant current and constant-MVA loads. The effect of the non-linear loads are reflected at the internal nodes of the generators as injected currents. The network nodes, including the load buses, are all Kron-reduced and the energy functions for the individual machines are obtained.

The validity of this modified model has been tested by assessing the transient stability of two test networks. Two sets of critical clearing times are obtained for each set of system conditions (e.g., fault location, non-linear load composition, etc.). One set corresponds to the results obtained by the method presented in this dissertation and the other one to the results obtained by time solution using a conventional transient stability computer program. Observations are made based on the comparison of the results. It is hoped that the presented results and observations would shed more light as well as confidence on the issue of load modeling in transient stability studies.

### III. MULTIMACHINE POWER SYSTEM REPRESENTATION

#### A. Classical Model with System Loads as Injected Currents

For digital simulation of the power system in dynamic studies a model is used which is valid for the duration as well as the specific purpose(s) of the study. In particular, when the simulation is performed to investigate the first-swing transient stability characteristics of the power network the so-called classical model is considered adequate for that purpose.

The set of assumptions employed in arriving at this model are listed below (Also see Chapter II of [32]).

- . Constant mechanical power input to each generator.
- . Transmission network is modeled by the steady state equations.
- . Synchronous machine represented by constant voltage behind direct axis transient reactance.
- . Damping is negligible.



- . The rotor angle of a machine coincides with the angle of the voltage behind the transient reactance.
- . Loads are represented by constant shunt impedances.

After a careful review of this list it was felt that the assumption regarding the representation of the loads is the most suspected one in the classical model.

Studies have shown that sizeable voltage fluctuations follow a major disturbance and at some buses voltages can dip to 0.5 per unit, even in stable cases. The transient voltage-MVA relationships of the loads are masked by the constant impedance model. This is an important issue which must not be overlooked in determining the transient behavior of the generator rotors.

It has been reported in the literature that the response of nearly all loads to voltage changes can be represented by some combination of constant impedance, constant current and constant-MVA devices depending on the nature and composition of the load [5]. Subsequently, it was concluded that, in transient stability studies, representation of individual loads by such combination would

be more realistic and would improve the results obtained by first swing transient stability assessment.

In the following derivation, the components of the power system, except for the loads, are represented by the classical model. To incorporate the effect of the non-linear loads (i.e., the constant current or the constant-MVA portion of the load) the nodes within the power network have been divided into three groups. The first group includes the generators' internal nodes (n); the second one contains load buses with "mixed" or non-linear load combination (m); and the last group includes the rest of the transmission network along with linear load buses (i.e., those buses with constant impedance loads only) (r).

Let  $\underline{I}_N$ ,  $\underline{I}_M$  and  $\underline{I}_R$  be the vector of node currents at the internal generator nodes, non-linear buses and the passive network nodes respectively. The corresponding node voltages are  $\underline{V}_N$ ,  $\underline{V}_M$  and  $\underline{V}_R$ . These node currents and voltages are related by the network's admittance matrix which is of the order (n+m+r). Partitioning this Y-matrix, the following relation could be obtained:

$$\begin{bmatrix} \underline{I}_N \\ \underline{I}_M \\ \underline{I}_R \end{bmatrix} = \begin{bmatrix} \underline{Y}_{NN} & \underline{Y}_{NM} & \underline{Y}_{MR} \\ \underline{Y}_{MN} & \underline{Y}_{MM} & \underline{Y}_{MR} \\ \underline{Y}_{RN} & \underline{Y}_{RM} & \underline{Y}_{RR} \end{bmatrix} \begin{bmatrix} \underline{V}_N \\ \underline{V}_M \\ \underline{V}_R \end{bmatrix} \quad (3.1)$$

where each submatrix of the Y-matrix (e.g.,  $\underline{Y}_{NN}$ ,  $\underline{Y}_{MR}$ , etc.) represents the mutual admittances as seen by any pair of nodes either within the same group or from two different groups.

Since there are no current injections at the passive nodes (i.e.,  $\underline{I}_R = \underline{0}$ ), these nodes could be eliminated by Kron reduction to obtain the following:

$$\begin{bmatrix} \underline{I}_N \\ \underline{I}_M \end{bmatrix} = \begin{bmatrix} \hat{\underline{Y}}_{NN} & \hat{\underline{Y}}_{NM} \\ \hat{\underline{Y}}_{MN} & \hat{\underline{Y}}_{MM} \end{bmatrix} \begin{bmatrix} \underline{V}_N \\ \underline{V}_M \end{bmatrix} \quad (3.2)$$

where the Symbol  $\hat{\underline{Y}}$  is used for the Y-matrix obtained by the reduction procedure.

The reduced network, described by equation (3.2), is schematically shown in Figure 3.1.

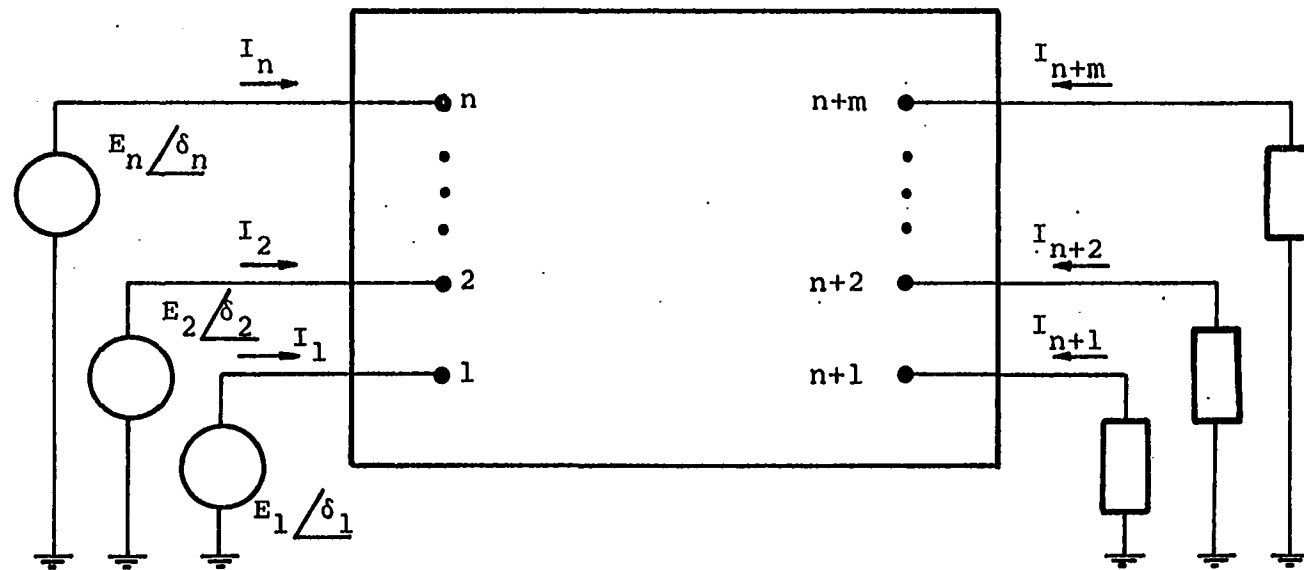


Figure 3.1. Reduced network after elimination of passive nodes

The currents  $I_{n+1}, I_{n+2}, \dots, I_{n+m}$  represent the non-linear load currents.

Let node  $j$  be a non-linear load bus with voltage  $V_j / \theta_j$ . Let the scheduled real and reactive power at node  $j$  be  $P_{Lj}$  and  $Q_{Lj}$ . The subscript LI is used to denote the constant current component of the load, and the subscript LM is used for the constant-MVA component of the load. Thus

$$P_{Lj} + jQ_{Lj} = (P_{LIj} + jQ_{LIj}) + (P_{LMj} + jQ_{LMj}) \quad (3.3)$$

where

$P_{LIj}$  : constant current real power at the  $j$ th node.

$P_{LMj}$  : constant-MVA real power at the  $j$ th node.

$Q_{LIj}$  : constant current reactive power at the  $j$ th node.

$Q_{LMj}$  : constant-MVA reactive power at the  $j$ th node.

The total current into the non-linear load node  $j$  will also be made up of two components corresponding to the constant current and constant-MVA portions of the load. This current is given by

$$-I_j \angle C_j = C_{Ij} + C_{Mj} \quad (3.4)$$

$j = n+1, \dots, n+m$

where

$$C_{Ij} = (P_{LIj} - j Q_{LIj}) / (V_j|_{t=0^-} \angle^{-\theta_j})$$

and

(3.5)

$$C_{Mj} = (P_{LMj} - j Q_{LMj}) / (V_j|_{t=0^+} \angle^{-\theta_j})$$

where

$C_{Ij}$ : Injected current due to constant current portion of the load at the  $j$ th node.

$V_j|_{t=0^-}$ : Magnitude of the pre-fault voltage at node  $j$ .

$V_j|_{t=0^+}$ : Magnitude of the  $j$ th node voltage at the start of the faulted period.

$\theta_j$ :  $j$ th node angle at the start of the faulted period.

$C_{Mj}$ : Injected current due to constant-MVA portion of the load at the  $j$ th node.

$$\text{Defining } \underline{C}^T = [C_{n+1}, C_{n+2}, \dots, C_{n+m}] \quad (3.6)$$

and comparing equation (3.2) and (3.4), it is noted that

$$\underline{I}_M = -\underline{C}$$

Eliminating  $\underline{V}_M$  from equation (3.2)

$$\underline{I}_N = [\underline{Y}_{NN} - \hat{\underline{Y}}_{NM} \hat{\underline{Y}}_{MM}^{-1} \hat{\underline{Y}}_{MN}] \underline{V}_N - \hat{\underline{Y}}_{NM} \hat{\underline{Y}}_{MM}^{-1} \underline{C} \quad (3.7)$$

$$\underline{I}_N = \tilde{\underline{Y}}_{NN} \underline{V}_N - \underline{K}_N$$

where

$$\tilde{\underline{Y}}_{NN} = \underline{Y}_{NN} - \hat{\underline{Y}}_{NM} \hat{\underline{Y}}_{MM}^{-1} \hat{\underline{Y}}_{MN} \quad (3.8)$$

$$\underline{K}_N = \hat{\underline{Y}}_{NM} \hat{\underline{Y}}_{MM}^{-1} \underline{C}_M = [K_1 \underline{\tau}_1, K_2 \underline{\tau}_2, \dots, K_n \underline{\tau}_n]^T$$

Equation (3.7) expresses the generator currents in terms of the internal generator node voltages  $\underline{V}_N$  and current injections  $\underline{K}_N$  that reflect the effect of the non-linear load currents.

#### B. Procedure for the Calculation of the Injected Load Currents

In the previous section, the modified model of the power system was presented. An important feature of this model is the absence of the network dependent variables (i.e., load bus voltages and angles) in the generator current equations, as shown in equation (3.7). However,

from equation (3.5), the non-linear load bus voltages are updated at the instant the disturbance (e.g., fault) is applied. Therefore, it seems obvious that the non-linear load current injections in equation (3.5) must reflect the transient variation of complex load bus voltages by a reasonable approximation.

It has been suggested that there are two types of voltage dips during most disturbances which threaten stability (E. W. Kimbark, discussion in [6]). One is called "fault dip" which is caused by a short circuit. Fault dips are generally characterized by a short duration and a sudden decrease of voltage followed by a sudden increase. The second type is called the "swing dip" It can be identified by slowly varying voltages and longer duration. Noting that the non-linear load models are adopted for the purpose of first swing transient stability analysis, the swing dips are justifiably ignored. On the other hand, a single network solution of the faulted network is all that is necessary to approximate the fault dips.<sup>1</sup>

Another important aspect of the non-linear load models involves the question of the individual load's power-factor. Digital simulation programs such as Philadelphia-

---

<sup>1</sup>This is a network solution performed at  $t = 0.00^+$ , or instantly after the disturbance has occurred.



Electric Company's (PECO) power system stability program maintain the pre-fault scheduled power factor for the entire duration of the disturbance [37]. This is true for both constant current as well as constant-MVA loads.

Based on the above arguments, two network solutions are performed before non-linear current injections are calculated. A network solution immediately after the occurrence of the disturbance (i.e., at  $t = 0.00^+$ ) will be used to calculate the non-linear load injected currents during the disturbance, and another solution reflecting all the post-disturbance changes in the network, will assist in calculation of the load currents which are valid for the post-disturbance period.

#### IV. TRANSIENT STABILITY ANALYSIS USING INDIVIDUAL ENERGY FUNCTIONS MODIFIED FOR NON-LINEAR LOADS

##### A. System Dynamic Equations In a Multimachine Power System

It was discussed earlier (Section B of Chapter II) that a common feature of direct methods is the development of a special function from which the stability characteristics of the system's post-disturbance equilibrium point is examined. The special function developed in this chapter is the individual machine energy function, first introduced by Vittal [2] and Michel et al. [3], which is being modified to represent the effect of the non-linear load models.

Modification of the individual machine energy function has found its origin in equation (3.7), where for each generator  $i$ , with its internal voltage  $E_i/\delta_i$ , the component of the non-linear load injected current is designated by  $K_i/\tau_i$ . From (3.7), the total current drawn at node  $i$  is given by

$$I_i = \sum_{N=1}^n \tilde{Y}_{iN} V_N - K_i \quad (4.1)$$

The electrical power of this generator is

$$P'_{ei} = R_e [E_i I_i^*] = E_i^2 G_{ii} + \sum_{\substack{j=1 \\ j \neq i}}^n [C_{ij} \sin \delta_{ij} + D_{ij} \cos \delta_{ij}] - E_i K_i \cos (\delta_i - \tau_i) \quad (4.2)$$

where

$$Y_{ij} = G_{ij} + j B_{ij}$$

$G_{ij}$ : Transfer conductance between node  $i$  and node  $j$ .

$B_{ij}$ : Transfer susceptance between node  $i$  and node  $j$ .

$$D_{ij} = E_i E_j G_{ij}$$

$$C_{ij} = E_i E_j B_{ij}$$

The set of system equations are given by

$$M_i \dot{\omega}_i = P_i - P_{ei}$$

$$\dot{\delta}_i = \omega_i \quad i = 1, 2, \dots, n \quad (4.3)$$

$$P_{ei} \triangleq \sum_{\substack{j=1 \\ j \neq i}}^n [C_{ij} \sin \delta_{ij} + D_{ij} \cos \delta_{ij}] - K_i E_i \cos(\delta_i - \tau_i)$$

where

$$P_i \triangleq P_{mi} - E_i^2 G_{ii}$$

$P_{mi}$ : Mechanical power of generator  $i$ .

$G_{ii}$ : Driving point conductance at node  $i$ .

$M_i$ : Inertia constant of generator  $i$ .

$\omega_i$ : Generator  $i$  rotor speed ( $\omega$ .r.t. a synchronous reference frame.)

Equation (4.3) expresses the motion of the generators with respect to an arbitrary synchronously rotating reference frame. A change of reference to the Center of Inertia (COI) coordinates will result in an individual machine energy function free of that component of energy responsible for the acceleration of the fictitious COI. This formulation has the advantage of removing the component of transient energy not responsible for pulling the respective machine away from the rest of the system.

The coordinates of the COI are defined by:

$$\delta_0 = \frac{1}{M_T} \sum_{i=1}^n M_i \delta_i$$

$$\omega_0 = \frac{1}{M_T} \sum_{i=1}^n M_i \omega_i \quad (4.4)$$

where

$$M_T = \sum_{i=1}^n M_i$$

The generator angle  $\theta$  and  $\tilde{\omega}$ , in the new coordinates are

$$\theta_i = \delta_i - \delta_0 \quad (4.5)$$

$$\tilde{\omega}_i = \omega_i - \omega_0$$

The system dynamic equations, in the COI reference frame, now become

$$M_i \ddot{\theta}_i = P_i - P_{ei} - \frac{M_i}{M_T} P_{COI}$$

$$\dot{\theta}_i = \tilde{\omega}_i \quad i = 1, 2, \dots, n \quad (4.6)$$

where

$$P_{COI} = M_T \dot{\omega}_0$$

$$\begin{aligned}
&= \sum_{i=1}^n P_i - 2 \sum_{i=1}^{n-1} \sum_{j=i+1}^n D_{ij} \cos \theta_{ij} + \sum_{i=1}^n E_i K_i \cos (\theta_i - \tau_i) \\
&\qquad\qquad\qquad i = 1, 2, \dots, n
\end{aligned} \tag{4.7}$$

### B. Transient Behavior of the Non-Linear Load Bus Angles

In a multimachine power system the motion of the center of inertia is influenced by the non-linear loads within the system, as indicated by the last group of terms in equation (4.7). It was also pointed out earlier that by performing a network solution at  $t = 0.00^+$ , the fast and sudden fault dips are accounted for.

In the following, an important assumption is made regarding the transient behavior of the non-linear load bus angles. This assumption is made due to the reduced formulation of equation (4.6), which is independent of the network dependent variables ( i.e., Non-linear load bus voltages and angles).

The assumption states that the motion of a non-linear load bus angle is assumed to coincide with the motion of a fictitious internal node angle of a generator with zero inertia and located at the same bus. Again, it is based on this assumption that a single set of  $K_i$ 's and  $\tau_i$ 's are satisfactory for each switching in the system.

C. Individual Machine Transient Energy Function  
with Non-Linear Loads.

The individual machine energy function for machine  $i$ ,  $V_i$ , is obtained by carrying out the following steps [2].

- . Rearrange equation (4.6)

$$M_i \ddot{\omega}_i - P_i + P_{ei} + \frac{M_i}{M_T} P_{COI}$$

- . Multiply by  $\dot{\theta}_i$

$$(M_i \ddot{\omega}_i - P_i + P_{ei} + \frac{M_i}{M_T} P_{COI}) \dot{\theta}_i$$

- . Integrate with respect to time. The coordinates of the post-disturbance stable equilibrium point ( $\theta^S, \omega^S = 0$ ) are used as the lower limit of integration.

$$V_i = 1/2 M_i \dot{\omega}_i^2 - P_i (\theta_i - \theta_i^S) + \int_{\theta_i^S}^{\theta_i} \left\{ \sum_{\substack{j=1 \\ \neq i}}^n [C_{ij} \sin \theta_{ij} + D_{ij} \cos \theta_{ij}] \right.$$

$$\left. - E_i K_i \cos (\theta_i - \tau_i) \right\} d\theta_i + \frac{M_i}{M_T} \int_{\theta_i^S}^{\theta_i} P_{COI} d\theta_i \quad (4.8)$$

$$i = 1, \dots, n$$

Finally, numerical integration of equation (4.8) can be performed using the Trapezoidal rule (see section B of Chapter IV).

$$\begin{aligned}
 V_i = & 1/2 M_i \dot{\omega}_i^2 - P_i(\theta_i - \theta_i^S) + \frac{1}{2} (\theta_i - \theta_i^S) \left\{ \sum_{\substack{j=1 \\ j \neq i}}^n [C_{ij} \sin \theta_{ij} + D_{ij} \cos \theta_{ij}] \right. \\
 & + \sum_{\substack{j=1 \\ j \neq i}}^n [C_{ij} \sin \theta_{ij}^S + D_{ij} \cos \theta_{ij}^S] - E_i K_i \cos (\theta_i - \tau_i) \\
 & \left. - E_i K_i \cos (\theta_i^S - \tau_i^S) \right\} \\
 & + \frac{M_i}{2M_T} (\theta_i - \theta_i^S) [P_{COI} - P_{COI}^S] \quad i=1, \dots, n \quad (4.9)
 \end{aligned}$$

#### D. Physical Interpretation of $V_i$

The recent success enjoyed by the direct energy methods in transient stability assessment is believed to be due to the fact that in this approach the basis for evaluation is a tool that properly accounts for the machines' transient energy and where it resides during the transient. This relatively fresh approach to the problem of transient stability analysis not only replaces an analytical approach by a mathematical one it also, as predicted over a quarter of a century ago, "provides a basis for future theoretical



work in a field where empirical methods have hitherto been the rule" [16].

The physical interpretation for the components of the system energy function [27], and later of the individual machine energy function [2], form the foundation for the evaluation of the method.

The first term in equation (4.8) represents the transient kinetic energy of machine  $i$ . The remaining terms make up the potential energy (with respect to  $\theta^S$ ), the components of which are the change in rotor potential energy as well as the network's change in potential energy as viewed from the internal node of the respective machine. Thus, equation (4.8) can be written as

$$V_i = V_{KE_i} + V_{PE_i}$$

Examining this equation one must note that the transient energy of machine  $i$  depends on the post-disturbance network and the position and speed of machine  $i$  relative to the other machines in the system. Thus the components of transient energy of machine  $i$  vary along the system trajectories. However, as the machine moves away from the rest of the system, its kinetic energy is being converted into potential energy. Therefore, it will

continue to move away from the system until the kinetic energy, possessed at the instant the disturbance was removed, is totally absorbed by the network (i.e., converted to potential energy). When this takes place, the machine will move toward the rest of the system and stability is maintained. If the kinetic energy is not totally absorbed by the network the machine will continue to move away from the other machines losing synchronism in the process.

Based on the foregoing argument and on extensive number of simulations, the authors of references [2-3] have arrived at the following postulations:

- . If the magnitude of the disturbance is increased to the point where one (or a group) machine becomes critically unstable, the potential energy of the critical machine goes through a maximum before instability occurs.
- . This maximum potential energy signifies the energy absorbing capacity of the network, as viewed from the critical machine, and is essentially independent of the duration of the disturbance or the mode of instability. It also defines the critical value of the critical machine's energy upon which transient stability assessment is made

$$V_{i\text{critical}} = V_{PE_i(\text{max})} \mid \text{along trajectory}$$

For stability to be maintained the energy of machine  $i$  at the instant the disturbance is removed (or at the beginning of the post-disturbance period) must be less than  $V_{i\text{critical}}$ .

#### E. Transient Stability Assessment-Criterion and Procedure

The criterion for transient stability assessment was derived based on the comparison between the maximum potential energy (i.e., the critical energy) of the critical machine and the value of the total energy at the instant the disturbance is removed. For example, when the disturbance is a fault the energy at fault clearing is of interest. Determining  $V_i^C$  as the energy at fault clearing,

if  $V_i^C < V_{i\text{critical}}$ , the system is stable.

and

if  $V_i^C > V_{i\text{critical}}$ , the system is unstable.

Furthermore, it was proven that the above conditions are satisfied for each of the critical machines, and for the critical machines as a group [2-3].

In this dissertation the following procedure has been used for the assessment of transient stability.

Step 1: For the post-disturbance network, the stable equilibrium point  $\theta^S$  for the generators' internal angles (w.r.t. the COI) and the short circuit admittance matrix  $Y_{BUS}$ , with all the network nodes retained, are determined. In much of the results presented in this dissertation, the same  $\theta^S$  obtained for the constant impedance load model was used.

Step 2: The parameters of the non-linear loads, equation (3.5), are computed. This step requires two network solutions: for the faulted and post-fault systems. To maintain constant power factor, the angle at the load bus is updated. For a constant current load, the load bus voltage magnitude is held at its pre-fault value. For a constant-MVA load, the load bus voltage magnitude is updated as well.

Step 3: All parameters of equations (4.6) and (4.8) are computed  
(e.g.,  $C_{ij}$ 's,  $D_{ij}$ 's,  $K_i$ 's,  $\tau_i$ 's, etc)

Step 4: The swing equations (4.3) or (4.6) are integrated for a sustained fault (run long enough to reach  $V_{PE_i}(\max)$ ).

Step 5: For each time interval  $V_{KE_i}$ ,  $V_{PE_i}$ , and  $V_i$  are computed. The procedure used is outlined below:

$$V_i(t+\Delta t) = V_i(t) + \Delta V_i \Big|_t^{t+\Delta t}$$

where  $\Delta V_i \Big|_t^{t+\Delta t}$  is obtained using trapazoidal integration rule.

Step 6: By examining  $V_i$  and its components, the value of  $V_i$  critical =  $V_{PE_i}(\max)$  is determined and stored for the given disturbance.

Step 7: For a given disturbance, the values of  $\theta_i$  and  $\tilde{\omega}_i$  are obtained at the end of the disturbance (e.g., at fault clearing).

Based on these informations  $V_i|_{t_{cl}}$  is computed.

Step 8: Transient stability check. Machine  $i$  will be stable or unstable depending on whether  $V_i|_{t_{cl}}$  is less than or greater than  $V_i \text{ critical}$ , respectively. Note that for a group of more than one machine going unstable, the above criterion should hold for each machine in the group. In addition,  $V$  for the group should also exceed its value of the group  $V \text{ critical}$ .

## V. RESULTS

The procedure for the assessment of first swing transient stability of a multimachine power system using the transient energy of the individual machines was outlined in Chapter IV. In this chapter, this procedure is validated by digital simulation. For this validation, two systems, a small test network and a larger system representing a reduced version of the Iowa power system, were selected. The description of the two systems is presented below.

A special computer program has also been developed to compute the modified energy functions for the individual machines used in the transient stability assessment. A description of this program is given in section B, and a complete listing is given in the Appendix.

### A. Test Systems

#### 1. 4-generator, 11-bus system

This system, shown in figure 5.1, is a modified version of the 9-bus, 3-machine, 3-load system widely used in the literature (see Chapter II of [32]) and is referred to as the WSCC system. The generator data and the initial operating conditions, including the internal generator

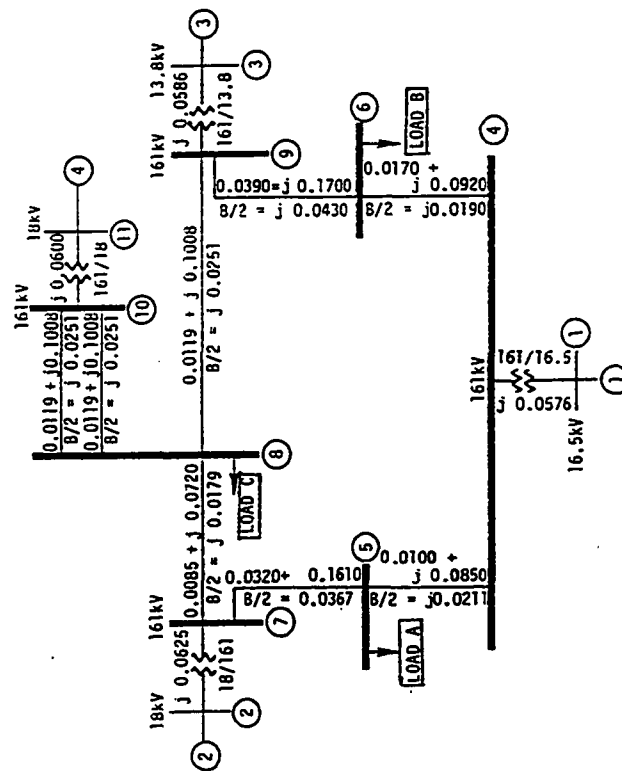


Figure 5.1. 4-generator test power system



voltages, are given in table 5.1. Three-phase faults at bus no. 10, near generator no. 4, have been studied for different load compositions and at the same load level. It is to be noted that the electrical load located at station C is very close to the fault, making its composition critical to the stability study results.

## 2. 17-generator, 163-bus modified Iowa system



This power system, shown in figure 5.2, is a reduced version of the principal power network of the state of Iowa. The development of the modified Iowa system has been described in reference [31]. The location of the major electrical loads with non-linear composition around the Eastern and Western parts of the state are also indicated in figure 5.2. The generator data and initial operating conditions, including the internal generator voltages, are also given in table 5.1.

The modified Iowa system was simulated in order to further investigate the effects of non-linear load representation on first swing transient stability characteristics. The disturbances investigated were three-phase faults in the vicinity of four major generation sites, located roughly along the western border of the state.

Table 5.1. Generator data and initial conditions

Generator Number	Generator Parameters <sup>a</sup>		Initial Conditions		
			Internal Voltage		
	H (MW/MVA)	$x_d^i$ (pu)	$P_{mo}^a$ (pu)	E (pu)	$\delta$ (degrees)
4-Generator System					
1	23.64	0.0608	2.269	1.0967	6.95
2	6.40	0.1198	1.600	1.1019	13.49
3	3.01	0.1813	1.000	1.1125	8.21
4	6.40	0.1198	1.600	1.0741	24.90
17-Generator System					
1	100.00	0.0040	20.000	1.0032	-27.92
2	34.56	0.0437	7.940	1.1333	-1.37
3	80.00	0.0100	15.000	1.0301	-16.28
4	80.00	0.0050	15.000	1.0008	-26.09
5	16.79	0.0507	4.470	1.0678	-6.24
6	32.49	0.0206	10.550	1.0505	-4.56
7	6.65	0.1131	1.309	1.0163	-23.02
8	2.66	0.3115	0.820	1.1235	-26.95
9	29.60	0.0535	5.517	1.1195	-12.41
10	5.00	0.1770	1.310	1.0652	-11.12
11	11.31	0.1049	1.730	1.0777	-24.30
12	19.79	0.0297	6.200	1.0609	-10.10
13	200.00	0.0020	25.709	1.0103	-38.10
14	200.00	0.0020	23.875	1.0206	-26.76
15	100.00	0.0040	24.670	1.0182	-21.09
16	28.60	0.0559	4.550	1.1243	-6.70
17	20.66	0.0544	5.750	1.1116	-4.35

<sup>a</sup>On 100-MVA base.

: Major load in the east (50% constant Z, 30% constant MVA, 20% constant I)  
: Major load in the west (60% constant Z, 20% constant MVA, 20% constant I)

**Figure 5.2 17-generator system (Reduced Iowa System)**

Information regarding the nature of the disturbances are listed below.

Raun fault: Bus no. 372, cleared by opening line 372-193.

Council Bluffs fault: Bus no. 436, cleared by opening line 436-771.

Ft. Calhoun fault: Bus no. 773, cleared by opening line 773-779.

Cooper fault: Bus no. 6, cleared by opening line 6-774.

#### B. Computer Program

A computer program, presented in the Appendix, was developed for this dissertation. This program which is written in Fortran language, has the following main features:

The program inputs the system data (bus data, line data, transformer data, etc.) and computes the unreduced admittance matrix  $Y_{BUS}$ .

The  $Y_{BUS}$  matrix is reduced to the internal nodes twice. This is due to the fact that two sets of network parameters (i.e., transfer conductances,

transfer susceptances and non-linear load current injections) need to be computed. The first set is used in the system dynamic equations (swing equations) and therefore represents the disturbed network. The other set is used to form the individual machine energy equations and represents the post-disturbance network<sup>1</sup>. This computation involves the inversion of complex matrices (see equation (3.8)). The subroutines 'DECOMPOSE' and 'SOLVE' are written to perform the complex matrix inversion.

- Using the parameters of the disturbed network, the swing equations are numerically integrated via subroutine 'DVERK'. This subroutine was obtained from IMSL library, Iowa State University Computation Center.
- The rotor angles and speeds are computed to the center of inertia reference frame. Using the parameters of the post-disturbance network, the individual machine energy functions are then computed and stored for each time step. At the end

---

<sup>1</sup>It must be noted that it is the stability of the post-disturbance stable equilibrium point that is being investigated by the individual machine energy functions.

of each time interval  $\Delta t$ , individual machines kinetic energy  $V_{KE_i}(t+\Delta t)$  is directly computed (see equation 4.9). The change in individual machine's potential energy  $\Delta V_{PE_i}$  is obtained using the trapazoidal integration rule (see equation 4.9). The potential energy of the individual machines at the end of each time interval  $\Delta t$  is then updated.

$$V_{PE_i}(t+\Delta t) = V_{PE_i}(t) + \Delta V_{PE_i} \quad (5.1)$$

The total energy of the individual machine is computed as follows.

$$V_i(t+\Delta t) = V_i(t) + \Delta V_i \Big|_t^{t+\Delta t} \quad (5.2)$$

- This program is terminated after the potential energy of the critical machine has reached its peak. Based on the critical energy of the individual machines and the criterion of the stability discussed in Chapter IV, the shortest critical clearing time and the corresponding critical machine are directly determined from the output of the program.

### C. Model Accuracy

By determining the actual fault trajectory and using this information in evaluating the individual machine energy functions, reference [2] has reported critical clearing times that are in excellent agreement with those obtained by time solution.

In this dissertation, however, transient voltage fluctuations are approximated in order to incorporate voltage dependent load models. This approximation directly influences the behavior of the loads during the transient period and therefore influences the behavior of the faulted trajectories as well. To investigate the fairness of the new load models a simple test was performed. This test was to compare the rotor angles, during the transient period, obtained using the proposed non-linear load models with those obtained by time solution using a conventional transient stability program. Figures 5.3-5.6 illustrate the results of such test for all four fault locations studied on the modified Iowa system.

In Figures 5.3-5.6, generators' rotor angles versus time<sup>1</sup> are plotted for a period of 0.2-0.3 seconds. Each

---

<sup>1</sup>These curves are commonly called swing curves.

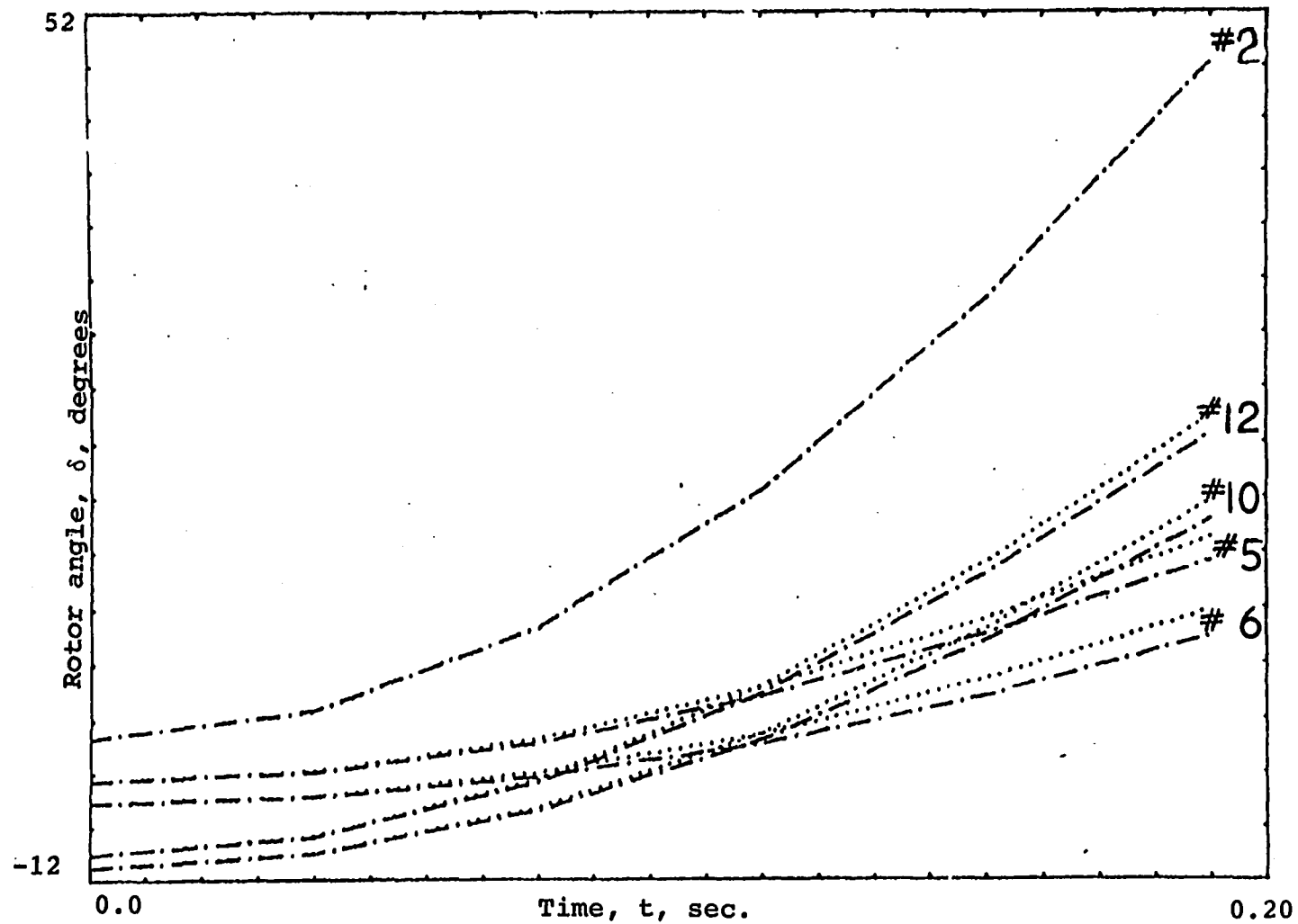


Figure 5.3. Comparison of faulted trajectories, fault at Cooper



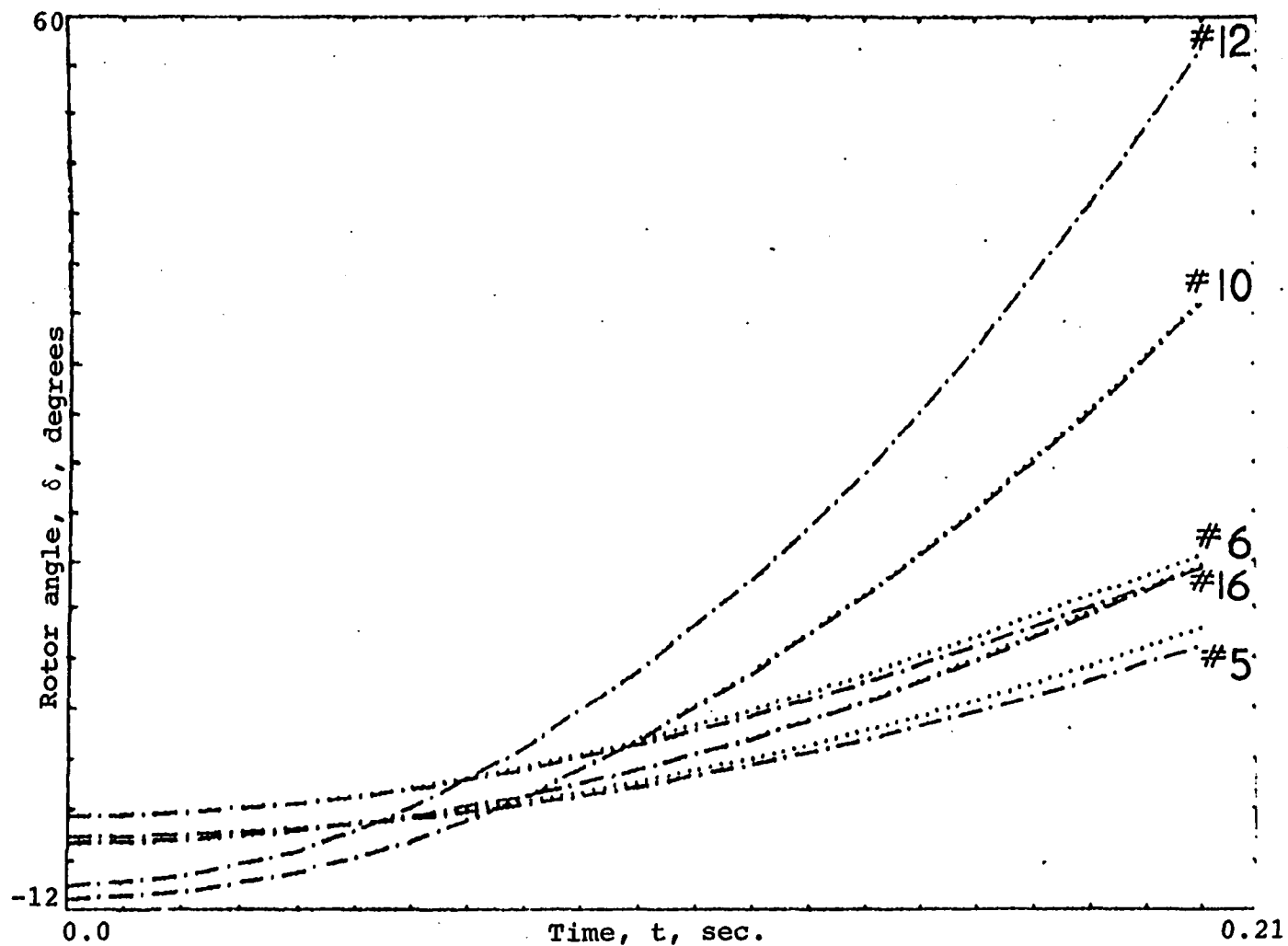


Figure 5.4. Comparison of faulted trajectories, fault at Council Bluffs

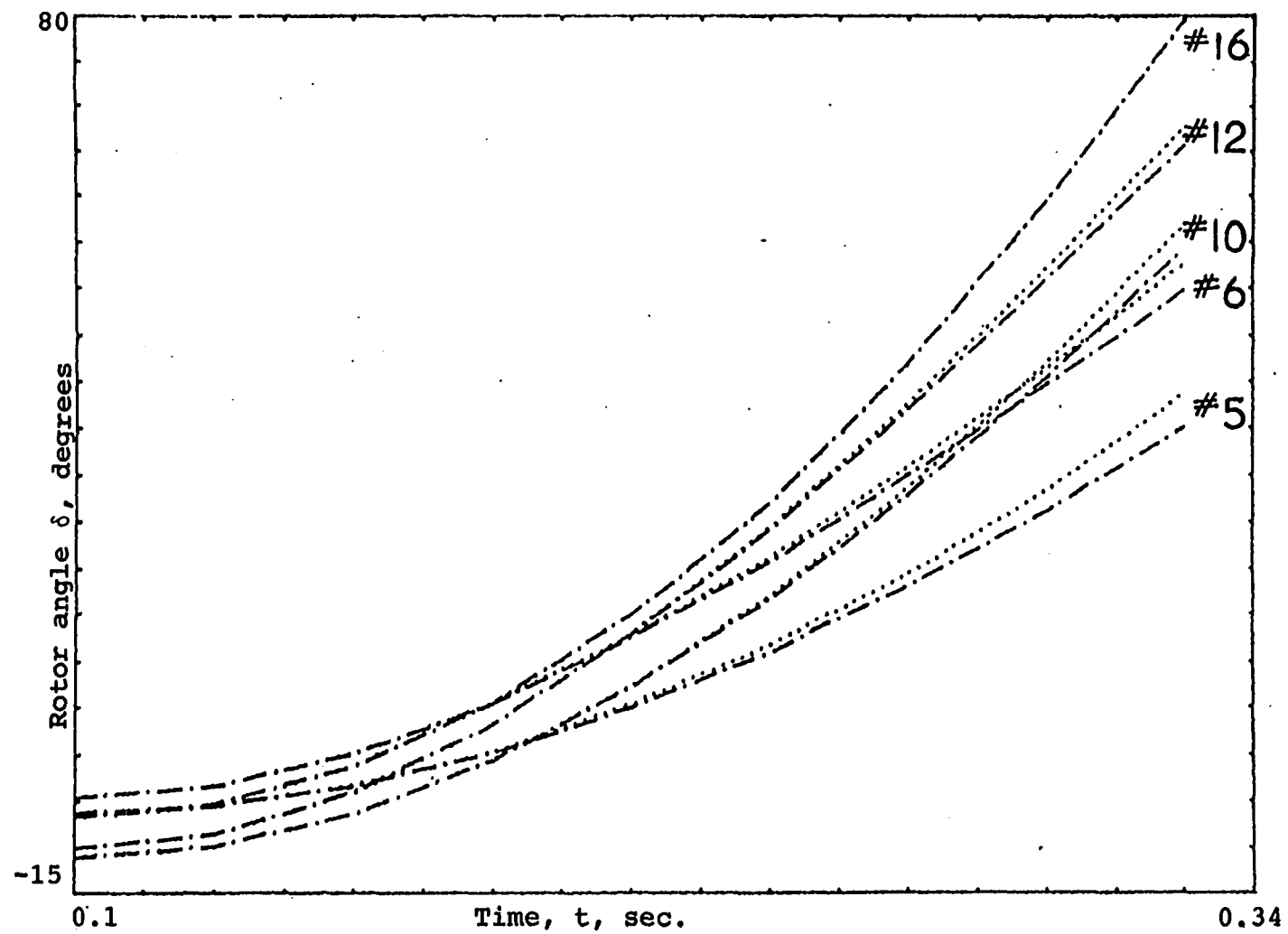


Figure 5.5. Comparison of faulted trajectories,  
fault at Ft. Calhoun

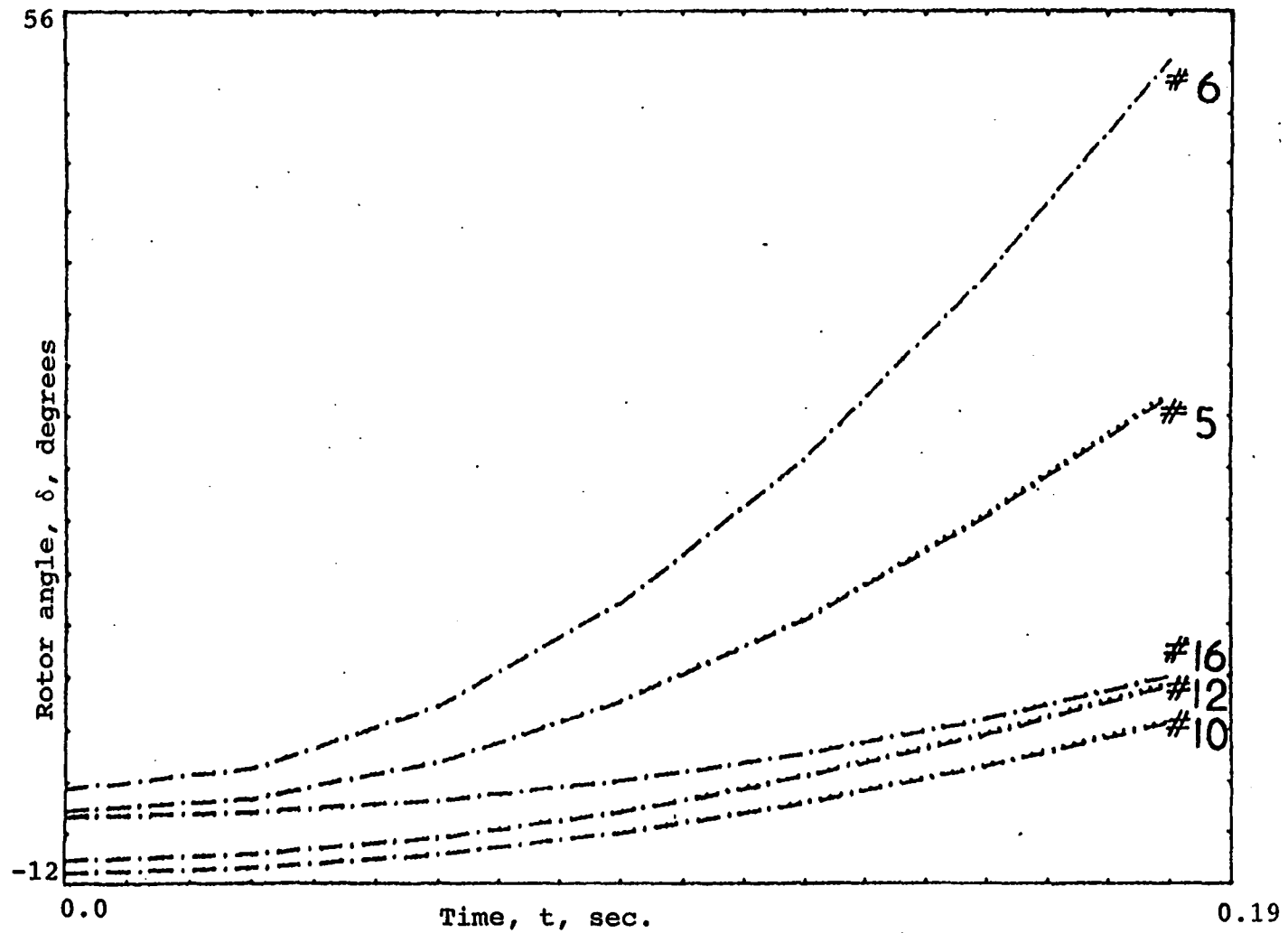


Figure 5.6. Comparison of faulted trajectories, fault at Raun

plot consists of two sets of curves, one obtained by the model used in this dissertation and another obtained by using Philadelphia Electric Company's (PECO) transient stability program [37]. Although identical model of power system is being used by both techniques, different methods of solution are employed. The PECO program performs simultaneous network solutions which allows the program to update load bus voltages and angles at every time interval. The method of this dissertation updates the same parameters only once, at the start of the transient period.

The close agreement between the two sets of trajectories in Figures 5.3-5.6 assures the fairness of the newly introduced load models adopted in this dissertation. It also supports the initial assumption that, for first swing transient stability characteristics, once the fast and sudden fault dips are accounted for, the slowly varying swing dips could be ignored.

Finally, it must be noted that the excellent agreement between the faulted trajectory of the generators adjacent to the fault by the two methods is due to the severe reduction of voltage near those generators (see equation (4.2)).

#### D. Stability Assessment

Prior to the development of this research, Vittal [2] and Michel et al. [3] had investigated the first swing transient stability characteristics of the two power networks presented earlier in this chapter for the same disturbances assuming constant shunt impedance representation of the loads. Subsequently, in order to investigate the influence of the newly modified load models on the previous results, several cases were selected. New load compositions and new non-linear load distributions in each case were selected to provide answers for such questions as:

The influence of non-linear load modeling on first swing transient stability characteristics as compared to those results previously obtained using linear load models.

The effects of non-linear load representation on the mode of instability.

The severity of constant-MVA loads versus constant current loads, especially near the fault where voltages are depressed the most.

The effects of the voltage dependent loads on the behavior and the pattern of potential and kinetic energy of the individual machines.

In each case, the components of the individual machine energy are calculated for each machine. For the critical machine(s), the critical energy, which is the same as  $V_{PE_i(max)}$ , is determined. The time at which, for the faulted trajectory, the total energy  $V_i$  equals this critical energy ( $V_{i,critical}$ ) is considered the critical fault clearing time, critical  $t_{c1}$ . This means that if stability is to be maintained, for the given fault and post-disturbance network, the fault duration must not exceed this value of critical  $t_{c1}$ .

#### 1. Stability assessment results

Data for stability assessment, based on the newly developed individual machine energy functions, are presented in table 5.2. For each of the two networks the following are given: The location of the disturbance (three-phase fault), the composition of the loads, the critical machines (i.e., the group of machines whose potential energy first reaches a maximum value), the value of  $V_{PE_i(max)}$  and the

Table 5.2  
Stability Assessment Using Individual Machine Energy Function

Case No.	Fault Location	Load Description	Critical Machine(s)	$V_{PEi \max}$	Critical $t_{cl,s}$ based on $V_{PEi \max}$
<u>4-Generator System</u>					
1.	bus #10	All loads const. I	#4	0.3565	0.120
2.	bus #10	Loads A,B: const. I			
		Load C: const. Z	#4	0.3414	0.129
3.	bus #10	Load A: const. MVA	#4	0.4237	0.1349
		Load B, C: const. Z			
4.	bus #10	Loads A, B: 60% const. Z	#4	0.4315	0.151
		20% const. I, 20% const. MVA			
		Load C: const. Z			
<u>17-Generator System</u>					
5.	Cooper	All loads const. I	#2	8.7733	0.202
6.	Cooper	Non-linear loads	#2	8.6928	0.205
		East + West			
7.	Ft. Calhoun	All loads const. I	#16	9.1818	0.346
8.	Ft. Calhoun	Non-linear loads	#16	9.7292	0.365
		East + West			
9.	Ft. Calhoun	Non-linear loads East only	#16	9.9565	0.360
		West loads: const Z			
10.	Council Bluffs	All loads const. I	#10,12	8.4506	0.186
11.	Council Bluffs	Non-linear loads	#10,12	10.4594	0.199
		East + West			
12.	Raun	All loads const. I	#5,6	12.7754	0.176
13.	Raun	Non-linear loads	#5,6	15.8284	0.188
		East + West			
14.	Raun	Non-linear loads East only	#5,6	16.4469	0.190
		West loads: const Z			

critical clearing time based on this value of  $V_{PE_i}(\max)$

For the cases listed in table 5.2, the critical clearing times were estimated using time solution obtained by the Philadelphia Electric Company's transient stability computer program; this clearing time was bracketed between a stable and an unstable cases. The estimated critical clearing times using  $V_{PE_i}(\max)$  and using time solution are tabulated and compared in table 5.3.

Examining the data in table 5.3, we note the close agreement between the critical clearing times obtained by the two methods. This agreement supports the validity of the technique suggested in this dissertation for the incorporation of non-linear voltage dependent load models in first swing transient analysis.

## 2. Effect of load model on transient stability

To investigate the effect of the non-linear load representation, the results in table 5.2 are compared with similar data for the same disturbances and networks using constant impedance load models. The latter data are obtained from reference [2] and are reproduced here in table 5.4.

Examining the data in table 5.2 and 5.4, we observe the following:



Table 5.3  
Comparison of Stability Assessment

Case No.	Fault Location	Critical $t_{cl,s}$ using $V_{PEi \max}$	Time solution - $t_{cl,s}$ stable	$t_{cl,s}$ unstable
<u>4-Generator System</u>				
1.	bus #10	0.120	0.100	0.110
2.	bus #10	0.124	0.120	0.130
3.	bus #10	0.134	0.130	0.135
4.	bus #10	0.151	0.143	0.146
<u>17-Generator System</u>				
5.	Cooper	0.202	0.200	0.202
6.	Cooper	0.205	0.200	0.210
7.	Ft. Calhoun	0.346	0.335	0.338
8.	Ft. Calhoun	0.365	0.350	0.355
9.	Ft. Calhoun	0.360	0.352	0.356
10.	Council Bluffs	0.186	0.192	0.193
11.	Council Bluffs	0.199	0.200	0.202
12.	Raun	0.176	0.180	0.182
13.	Raun	0.188	0.184	0.188
14.	Raun	0.190	0.190	0.195

Table 5.4  
Stability Assessment Using Individual Machine Energy Function<sup>a</sup>

Case No.	Fault Location	Load Description	Critical Machine(s)	$V_{PEi \max}$	Critical $t_{cl,s}$ based on $V_{PEi \max}$
<u>4-Generator System</u>					
1	bus #10	All loads const. Z	#4	0.6420	0.1572
<u>17-Generator System</u>					
2	Cooper	All loads const. Z	#2	11.0437	0.210
3	Ft. Calhoun	All loads const. Z	#16	12.2501	0.350
4	Council Bluffs	All loads const. Z	#12	11.5305	0.202
5	Raun	All loads const. Z	#5,6	18.4312	0.1923

<sup>a</sup>Reported from reference [2].

1. The energy absorbing capacity of the network as viewed by internal node of the critical machine(s),  $V_{PE_i}(\max)$ , is influenced by the location as well as the composition of the non-linear loads around the network. In other words, when voltage dependent, i.e., constant current or constant-MVA, loads replace the constant impedance loads the transient characteristics of the power network are changed. For example, we note that the values of  $V_{PE_i}(\max)$  for the cases in table 5.2 are consistently lower than the values of the corresponding cases listed in table 5.4.

2. The obtained critical clearing times are also dependent upon the choice of the load models. In fact, the critical clearing times obtained in table 5.2 were almost always shorter than the corresponding results from table 5.4 (where all loads are represented by constant impedance model). This means that, for those cases studied in this chapter, the linear representation of the loads leads to optimistic results. However, this may not always be true. There are situations where constant impedance representation of the load might lead to optimistic results (e.g., compare case no. 8 with case no. 9, both in table 5.2). The important point is that the constant impedance load representation masks the transient voltage fluctuations and may give an unrealistic picture of the power network.

3. The mode of stability is independent of the choice of the load models. This means that, for the different load combinations studied in table 5.2, the critical machine(s) stays the same even when its critical energy and its critical clearing time do not.

### 3. Two sources of error

Finally, while performing digital simulation on the test networks, two sources of error were detected.

1. When the disturbance is at (or near) one of the two machines at the same plant (e.g., two machines at Raun in the modified Iowa network), transient stability assessment of the system can be correctly made based on  $V_{PE_i}(\max)$  for the "dominant" machine, or even based on the critical energy of the equivalent of the two machines. However, when critical energy of the second machine alone is used for assessment, the results are not as reliable. The reason appears to be that the individual machine's energy function for the dominant machine is so much greater than that of the second machine that the generator's current injections, due to the non-linear loads, may tend to distort the values of  $V_i$  for the two closely coupled machines.

2. The value of the post-disturbance stable equilibrium points used in the dissertation are those obtained using constant impedance load models, as in reference [2]. To explore how dependent this choice is on the particular load models used, a new set of angles were obtained using a succession of load flow runs for the Raun fault holding the generators' powers constant. The new values obtained by this procedure differed only slightly from the previous values. New cases 12-14 were run, where  $V_{PE_i}(\max)$  were computed using the new angles. However, the newly computed critical energies, and the corresponding critical clearing times, were essentially the same as those in table 5.2.

## VI. CONCLUSIONS

In 1982, Fouad and Vittal [2,3] proposed a criterion for direct assessment of first swing transient stability based on the individual machine energy functions. Using the classical model of the power system, they obtained critical fault clearing times that were in excellent agreement with those obtained by time solution. In all cases, the mode of instability was correctly predicted, even in very complex situations.

A major shortcoming of the above work has been the constant impedance representation of the electrical loads. This linear model of the loads is an unrealistic model because it masks the transient voltage fluctuations that follow the disturbance.

The major objectives of this dissertation have been:

1. To replace the linear model of the loads by a more realistic one which accounts for the transient voltage changes and to develop a new expression for the individual machine energy function which incorporates the new load model.

2. To investigate the effects of the modified load representation on first swing transient stability characteristics of the power system.

Efforts and accomplishments concerning the research objectives have been presented in the previous chapters. Subsequently, two sets of conclusions are drawn. First, conclusions are made based on the issue of proper load representation in stability studies. Secondly, conclusions are drawn based on the results presented in Chapter V.

A. Conclusions Drawn Based on Proper Representation of Loads in Stability Studies

1. Proper representation of loads as a function of voltage and frequency is important in power systems stability studies.
2. Load modeling is a difficult task due to the stochastic nature of the loads. Individual loads exhibit different characteristics. These characteristics are dependent on such complex factors as time of the day, weather, human use patterns, etc.

3. In power system stability studies, it is not necessary to know the behavior of each individual load device. Only the aggregate behavior of the power system load is desired.
4. When the classical model of power system is used, loads are represented as constant impedances. This linear model of the loads masks the true nature of voltage changes following a disturbance.
5. A more realistic model of the voltage dependent loads is the one that either accounts for the transient voltage fluctuations directly or a model that approximates the transient voltage changes, as is the case in this dissertation. It is important to note that the order of network formulation is directly related to this choice.

#### B. Conclusions Drawn Based on the Results of Chapter V

1. A more realistic model of load is proposed. In this model, loads are represented by any desired combination of constant impedance, constant current or constant-MVA



models. The effect of the non-linear loads is reflected at the internal nodes of generators as injected currents.

2. Transient voltage fluctuations are successfully approximated by using only the network information at the start of the transient period. This approximation technique accounts for the fast and sudden fault dips and ignores the slowly varying swing dips. Since there is no need to continuously update the voltages, load buses are Kron reduced and an internal node representation of the power system is derived.
3. It was found that the faulted trajectories obtained using the proposed non-linear load models were in good agreement with the ones obtained by time solution using the Philadelphia Electric Company's (PECO) transient stability program. This comparison assured the fairness of the proposed load model.
4. Criterion of stability suggested in references [2,3] was found to be valid, even when constant impedance loads were replaced by voltage dependent constant current or constant-MVA loads. Nevertheless, the peak

of the potential energy reached by the critical machine(s) is influenced by the presence of the non-linear load models. This effect has the following consequences:

First, the properties of the power network are closely coupled to the voltage characteristics of the loads. Secondly, the critical energy or the energy absorbing capacity of the network as viewed by the internal node of the critical machine(s) is also dependent on the choice of the load models.

5. Critical fault clearing times, or the time at which the critical machine's total energy reaches its critical energy, is also influenced by the voltage characteristics of the loads. In almost all cases studied, the obtained critical fault clearing times were reduced as a result of replacing linear load models by non-linear load models.

However, it is not always clear whether pessimistic or optimistic results should be expected. Constant impedance representation of the loads might indicate a more stable system in one case while it might indicate a less stable system in another. The same is true for non-linear voltage dependent loads

such as constant current or constant-MVA loads. the primary difference is that the results obtained using non-linear load models are more realistic and therefore tend to reflect the true system response.

6. The machines tending to lose synchronism seem to be independent of the voltage characteristics of the loads. However, depending on the characteristics of the power system and also depending on the nature of the disturbance, there exists a possibility of a situation where the mode of instability will be dependent on the model of the loads.
7. The critical fault clearing times obtained using the modified individual machine energy functions were found to be in close agreement with the corresponding time solution results obtained using the Philadelphia Electric Company's (PECO) transient stability program. However, the two sets of results are not identical. This is due to the fact that in the method of this dissertation the transient voltage fluctuations are approximated while the same voltages are continuously updated (no approximation) in the other method. It must be noted that the mismatch between the two sets of results vanishes as all loads are represented by the linear model.

## VII. REFERENCES

1. Fouad, A. A. "Stability theory-Criteria for Transient Stability." Proceedings, Conference on Systems Engineering for Power: Status and Prospects, (Henniker, N.H.) Publication No. CONF-750867, (1975): 421-450.
2. Vittal, V. "Power System Transient Stability using the Critical Energy of Individual Machines." Ph.D. dissertation. Iowa State University, Ames, IA, 1982.
3. Michel, A. N., Fouad, A. A. and Vittal, V. "Power System Transient Stability Using Individual Machine Energy Functions." IEEE Transactions CAS-30 (May 1983): 266-276.
4. Ribeiro, J. R. and Lange, F. J. "A new Aggregation Method for Determining Composite Load Characteristics." IEEE Transactions PAS-101 (August 1982): 2869-2875.
5. Kent, M. H., Schmus, W. R., McCrackin, F. A. and Wheeler, L. H. "Dynamic Modeling of Loads in the Stability Studies." IEEE Transactions PAS-88 (May 1969): 760-765.
6. Illiceto, F., Ceyhan, A and Ruckstuhl, G. "Behavior of Loads during Voltage Dips Encountered in Stability Studies. Field and Laboratory Tests." IEEE Transactions PAS-91 (December 1972): 2470-2479.
7. "System Load Dynamics-Simulation Effects and Determination of Load Constants." IEEE Transactions PAS-92 (April 1975): 600-609.
8. Sabir, S. A. Y. and Lee, D. C. "Dynamic Load Models Derived from Data Acquired during System Transients." IEEE Transactions PAS-101 (September 1982): 3365-3372.
9. Vemuri, S., Hill, E. R., Balasubramanian, R. And Stanton, K. N. "Estimation of Power System Load Parameters in the Presence of System Disturbances." Paper A77-034-2. IEEE PES Winter Meeting, New York, NY, 1977.

10. Harrison, K. C. and Laskowski, T. F. "Transient Stability Sensitivity to Detailed Load Models: A Parametric Study." Paper A78-559-7. IEEE PES Summer Meeting, Los Angeles, CA, 1978.
11. Nguyen, C. T., Pannetor, J. G. Robichaud, Y. St. Jacques, A. and Scrinivasan, K. "Load Characteristics and the Stability of the Hydro-Quebec System." Paper A 79-438-3. IEEE PES Summer Meeting, Vancouver, British Columbia, 1979.
12. Concordia, C. and Ihara, S. "Load Representation in Power System Stability Studies." IEEE Transactions PAS-101 (April 1982): 969-977.
13. Concordia, C. "Representation of Loads." Symposium on Adequacy and Philosophy of Modeling: Dynamic System Performance. 75 CH 0970-4-PWR. IEEE PES Winter Meeting, New York, NY, 1975.
14. Criteria of Stability of Electric Power Systems. A report. Union Institute of Scientific and Technological Information and The Academy of Sciences of U.S.S.R. Electric Technology and Electric Power Services, Moscow, 1971. (in Russian).
15. Magnusson, P.C. "Transient Energy Method of Calculating Stability." AIEE Transactions PAS-66 (1947): 747-755.
16. Aylett, P.D. "The Energy Integral Criterion of Transient Stability Limits of Power Systems." Proceedings IEE, 105 (c) (1958): 527-536.
17. Gless, G. E. "Direct Method of Lyapunov Applied to Transient Power System Stability." IEEE Transactions PAS-85 (February 1966): 169-179.
18. El-Abiad, A. H. and Nagappan, K. "Transient Stability Regions of Multimachine Power Systems." IEEE Transactions PAS-85 (February 1966): 158-168.
19. Pai, M. A., Mohan, M. A. and Rao, J. G. "Power System Transient Stability Regions Using Popov's Method." IEEE Transactions PAS-89 (May/June 1970): 788-794.

20. Kitamura, S., Dohnomoto, T. and Kurematsu, Y. "Construction of a Lyapunov Function by the Perturbation Method and Its Application to the Transient Stability Problem of Power Systems with Non-Negligible Transfer Conductances." Int. J. of Control 26 (1977): 405-420.
21. Prabhakara, F. S. and El-Abiad, A. H. "A Simplified Determination of Transient Stability Regions for Lyapunov Methods." IEEE Transactions PAS-94 (March/April 1975): 672:689.
22. Gupta, C. L. and El-Abiad, A. H. "Determination of the Closest Unstable Equilibrium State for Lyapunov Methods in Transient Stability Studies." IEEE Transactions PAS-94 (September/October 1976): 1699-1712.
23. Ribbens-Pavella, M. "Transient Stability of Multimachine Power Systems by Lyapunov's Direct Method." Proceedings of Seminar on Stability of Large Scale Power Systems at the University of Liege, Liege, Belgium, 1972.
24. Athay, T., Podmore, R. and Virmami, S. "A Practical Method for Direct Analysis of Transient Stability." IEEE Transactions PAS-98 (1979): 573-584.
25. Athay, T. Sherket, V. R., Podmore, R., Virmani, S. and Puech, C. "Transient Energy Analysis." Proceedings Conference on Systems Engineering for Power: Emergency Operating State Control, Davos, Switzerland, 1979.
26. Tavora, C. J. and Smith, O.J.M. "Characterization of Equilibrium and Stability in Power Systems." IEEE Transactions PAS-91 (May/June 1972): 1127-1145.
27. Lugtu, R.L. and Fouad, A. A. "Transient Stability Analysis of Power Systems Using Lyapunov's Second Method." IEEE Conference Paper No. C721 45-6.
28. Uyemura, K., Matsuki, J., Yamada, I. and Tsuji, T. "Approximation of an Energy Function in Transient Stability Analysis of Power Systems." Electrical Engineering in Japan 92, No. 6 (Nov./Dec. 1972): 96-100.

29. Kakimoto, N., Ohsawa, Y. and Hayashi, M. "Transient Stability Analysis of Electric Power Systems Via Lure' Type Lyapunov Function." Proceedings of IEE (Japan) 98 (May/June 1978): 63-78.
30. Fouad, A. A. and Stanton, S. E. "Transient Stability Analysis of a Multi-Machine Power System. Part I: Investigation of System Trajectory, and Part II: Critical Transient Energy." IEEE Transactions PAS-100 (August 1981): 3408-3424.
31. Fouad, A. A. Kruempel, K. C., Mamandur, K. R. C., Pai, M. A. Stanton, S. E. and Vittal, V. "Transient Stability Margin as a Tool for Dynamic Security Assessment". EPRI Report No. EL-1755, March 1981.
32. Anderson, P. M. and Fouad, A. A. Power System Control and Stability. Vol. I. Ames, Iowa: The Iowa State University Press, 1977.
33. Bergen, A. R., and Hill, D. J. "A Structure Preserving Model for Power System Stability Analysis." IEEE Transactions PAS-100 (March 1981): 25-35.
34. Athay, T. M. and Sun, D. I. "An Improved Energy Function for Transient Stability Analysis." Proceedings of the International Symposium on Circuits and Systems, April 1981.
35. Pai, M. A., Padiyar, K. R. and Radhakrishna, C. "Transient Stability Analysis of Multimachine AC/DC Power Systems Via Energy Function Method." IEEE Transactions PAS-100 (December 1981): 5027-5035.
36. Narasimhamurthi, N. and Musavi, M. T. "Incorporating Load Voltage Fluctuations in Transient Stability Analysis Using Lyapunov's Second Method." Proceedings, Midwest Power Symposium, Madison, Wisconsin, 1982.
37. Power System Stability Program. User's Guide UG004-2. Philadelphia, PA.: Philadelphia Electric Co., System Planning Division, 1971.

## VIII. ACKNOWLEDGMENTS

I would like to express my heartfelt gratitude to my major professor Dr. A. A. Fouad for the time and attention he has devoted to me and to this work.

I would also like to thank Dr. V. Vittal for his sustained interest and support during this work. Special thanks are extended to the members of the committee for their valuable time and advice.

I am greatly indebted to my family for constantly encouraging me to set and attain high goals in my life.

Thanks are also extended to Roberta North for typing this thesis.



IX. APPENDIX: COMPUTER PROGRAMS

```

C THIS PROGRAM INPUTS BUS DATA, LINE DATA,
C TRANSFORMER DATA, PRE-FAULT LOAD FLOW DATA,
C GENERATOR PARAMETERS, FAULT LOCATION AND
C LINES CLEARED TO CALCULATE REDUCED FAULTED
C Y-BUS, POST-FAULT Y-BUS AND VOLTAGE AND
C ANGLE AT GENERATOR INTERNAL BUS.
C -----
      COMPLEX Y(170,170), E(170), VT(39), CT(39)
      COMPLEX YF, YR(120,120), Y1(40,40), Y2(40,40)
      COMPLEX YSHUNT, YIJ, ZIJ, YII, YJJ, CURR, S, EDP
      COMPLEX YFICT, SI(170), CI(170)
      COMPLEX YNMF(90,90), YMMF(90,90), YNMMF(90,90), BBF(90,90)
      COMPLEX CIF(40), EPF(170), CII(170), CM(170), CMM(170)
      COMPLEX DRP(90), DAVT(90), EFF(170), SM(170), CC(170), CCC(170)
      INTEGER TYPE(170), GBUS(170)
      DIMENSION PBASE(39), H(39), R(39), XD1(39), DAMP(39)
      DIMENSION OUT(39,6), PM(40), EF(40)
      DIMENSION FK(40), ALPHAF(40), LI(90)
C -----
C START READING DATA.
C -----
      READ(15,1000)NGEN,NI
1000  FORMAT(2I5)
C -----
C READ GENERATOR PARAMETERS.
C -----
      DO 20 I=1,NGEN
      READ(15,1010)PBASE(I),H(I),R(I),XD1(I),DAMP(I)
1010  FORMAT(8F10.4)
C      CONVERT THE DATA TO 100MW BASE
      C=100.0/PBASE(I)
      H(I)=H(I)/C
      R(I)=R(I)*C
      XD1(I)=XD1(I)*C
      DAMP(I)=0.0
20    CONTINUE
C -----
C THIS SEGMENT OF THE CODE PERFORMS THE FOLLOWING FUNCTIONS
C
C 1. FORMS 3 Y-BUS ARRAYS
C 2. REDUCES Y-BUSES TO INTERNAL NODES
C 3. CALCULATES GENERATOR INITIAL CONDITIONS
C -----
C INITIALIZE VARIABLES
      DO 10 I=1,170
      E(I)=(0.0,0.0)
      TYPE(I)=0
      DO 10 J=1,170
10    Y(I,J)=(0.0,0.0)
      READ(15,990)NBUS,NGEN

```

```

990     FORMAT(2I5)
C   LOOP HERE FOR EACH BUS
      N=0
      K=NGEN
16     READ(15,1001)I,NTYPE,EMAG,ARG,PLZ,QLZ,PG,QG,PLI,QLI,YSHUNT
1001   FORMAT(I5,T18,I1,F6.4,F6.2,6F6.1,T67,2F6.3)
      IF(I.EQ.0)GO TO 17
      IF(NTYPE.NE.2)GO TO 159
      READ(15,158)EMAGPF,ARGPF,PLM,QLM,EMAGF
158   FORMAT(T19,F6.4,F6.2,2F6.1,F6.4)
      ARGPF=ARGPF*3.14159/180.0
      EPF(I)=EMAGPF*CMPLX(COS(ARGPF),SIN(ARGPF))
      EFF(I)=EMAGF*CMPLX(COS(ARG),SIN(ARG))
159   ARG=ARG*3.14159/180.0
      Y(I,I)=Y(I,I)+YSHUNT+CMPLX(PLZ,-QLZ)*.01/EMAG**2
      TYPE(I)=NTYPE
      E(I)=EMAG*CMPLX(COS(ARG),SIN(ARG))
      SI(I)=CMPLX(PLI,QLI)*0.01
      SM(I)=CMPLX(PLM,QLM)*0.01
      CC(I)=CONJG(SI(I)/E(I))
      IF(NTYPE.NE.2)GO TO 164
      CCC(I)=CONJG(SI(I)/EPF(I))
      CM(I)=CONJG(SM(I)/EFF(I))
      CI(I)=CC(I)+CM(I)
      CMM(I)=CONJG(SM(I)/EPF(I))
      CII(I)=CCC(I)+CMM(I)
164   IF(TYPE(I).EQ.1)GO TO 18
      Y(I,I)=Y(I,I)+CMPLX(-PG,QG)*.01/EMAG**2
      IF(TYPE(I).EQ.2)GO TO 19
      GO TO 16
18     N=N+1
      GBUS(N)=I
      VT(N)=E(I)
      CT(N)=CMPLX(PG,QG)
      GO TO 16
19     K=K+1
      GBUS(K)=I
      GO TO 16
17     CONTINUE
      NGEN=N
C   LOOP HERE FOR EACH LINE TO BE READ
21     READ(15,1003)I,J,ZIJ,B
1003   FORMAT(2I5,3F10.5)
      IF (I.EQ.0)GO TO 25
      YIJ=(1.0,0.0)/ZIJ
      Y(I,I)=Y(I,I)+YIJ+CMPLX(0.0,B/2.0)
      Y(J,J)=Y(J,J)+YIJ+CMPLX(0.0,B/2.0)
      Y(I,J)=Y(I,J)-YIJ
      Y(J,I)=Y(J,I)-YIJ
      GO TO 21

```

```

25      CONTINUE
C      LOOP HERE FOR EACH TRANSFORMER CARD TO BE READ
30      READ(15,1004)I,J,ZIJ,RATIO
1004    FORMAT(2I5,2F10.5,F6.4)
        IF(I.EQ.0)GO TO 35
        YIJ=(1.0,0.0)/ZIJ
        YII=YIJ*(1.0/RATIO-1.0)/RATIO
        YJJ=YIJ*(1.0-1.0/RATIO)
        YIJ=YIJ/RATIO
        Y(I,I)=Y(I,I)+YII+YIJ
        Y(J,J)=Y(J,J)+YJJ+YIJ
        Y(I,J)=Y(I,J)-YIJ
        Y(J,I)=Y(J,I)-YIJ
        GO TO 30
35      CONTINUE
        DO 195 N=1,NGEN
        PG=REAL(CT(N))
        QG=AIMAG(CT(N))
        CT(N)=CONJG(CMPLX(PG,QG)/VT(N))
        CT(N)=CT(N)/100.
195      CONTINUE
        DO 1934 I=1,NBUS
        DO 1934 J=1,NBUS
        WRITE(11)Y(I,J)
1934     CONTINUE
C      -----
C      INITIALIZATION OF GENERATOR VARIABLES
C      CALCULATE VOLATAGE BEHIND TRANSIENT REACTANCE
C      -----
        DO 280 I=1,NGEN
        EDP=VT(I)+CMPLX(R(I),XD1(I))*CT(I)
        EF(I)=CABS(EDP)
        DEL=ATAN2(AIMAG(EDP),REAL(EDP))
        CURR=CT(I)
        CA=CABS(CT(I))
        CURR=VT(I)*CONJG(CT(I))
        PE=REAL(CURR)
        PE=PE+CA*CA*R(I)
        PM(I)=PE
        OUT(I,1)=0.0
        OUT(I,2)=DEL
        WRITE(16)I,EF(I),DEL,PE
280      CONTINUE
        READ(15,2000)NFAULT,JFAULT,YF
        KCOUNT=0
2000     FORMAT(2I5,2F10.4)
        REWIND 11
        DO 1939 I=1,NBUS
        DO 1939 J=1,NBUS
        READ(11) Y(I,J)

```

```

1939  CONTINUE
      DUM=CABS(YF)
      IF(DUM.GT.1.0E-08) GO TO 230
C     NO FAULT IMPEDANCE
C     ZERO ROW AND COLUMN AT THE FAULTED BUS
      IROW=NFAULT
      DO 38 I=1,NBUS
        Y(I,NFAULT)=(0.0,0.0)
        Y(NFAULT,I)=(0.0,0.0)
38    CONTINUE
      GO TO 39
230   Y(NFAULT,NFAULT)=Y(NFAULT,NFAULT)+YF
      GO TO 39
39    CONTINUE
C     PERFORM KRON REDUCTION
      DO 60 M=1,NBUS
        IF(M.EQ.IROW) GO TO 60
        IF(TYPE(M).EQ.1) GO TO 60
        IF(TYPE(M).EQ.2) GO TO 60
        IF(CABS(Y(M,M)).LT.1.0E-08)GO TO 60
        TYPE(M)=-1
        DO 50 I=1,NBUS
          IF(TYPE(I).EQ.-1)GO TO 50
        DO 40 J=1,NBUS
          IF(TYPE(J).EQ.-1)GO TO 40
          Y(I,J)=Y(I,J)-Y(I,M)*Y(M,J)/Y(M,M)
40    CONTINUE
50    CONTINUE
60    CONTINUE
      IROW=0
C     RESET TYPE FOR OTHER CALLS
      NGENI=NGEN+NI
      DO 65 I=1,NBUS
        IF(TYPE(I).EQ.1) GO TO 65
        IF(TYPE(I).EQ.2) GO TO 65
        TYPE(I)=0
65    CONTINUE
      DO 85 I=1,NGENI
        KK=GBUS(I)
        DO 83 K=1,NGENI
          KN=GBUS(K)
          YR(I,K)=Y(KK,KN)
83    CONTINUE
85    CONTINUE
C     AUGMENT Y-MATRIX WITH GENERATOR BUSES
C     ELIMINATE THE TERMINAL BUSES
      N1=NGEN+NI+1
      DO 80 I=1,NGEN
        YR(N1,N1)=YR(I,I)
        YR(I,I)=(0.0,0.0)

```

```

      DO 75 J=1,NGENI
      YR(N1,J)=YR(I,J)
      YR(I,J)=(0.0,0.0)
      YR(J,N1)=YR(J,I)
      YR(J,I)=(0.0,0.0)
75    CONTINUE
C    ADD IN GENERATOR BUS
      YFICT=CMPLX(R(I),XD1(I))
      YFICT=1./YFICT
      YR(I,I)=YFICT
      IF(CABS(YR(N1,N1)).EQ.0.0)GO TO 80
      YR(N1,N1)=YR(N1,N1)+YFICT
      YR(I,N1)=-YFICT
      YR(N1,I)=-YFICT
      DO 76 M=1,NGENI
      DO 76 N=M,NGENI
      YR(M,N)=YR(M,N)-YR(M,N1)*YR(N1,N)/YR(N1,N1)
      YR(N,M)=YR(M,N)
76    CONTINUE
80    CONTINUE
      IF(NI.EQ.0)GO TO 485
C    START PARTITIONING THE FAULTED Y-BUS
      NGENI=NGEN+NI
      DO 402 I=1,NGEN
      KK=NGEN+1
      DO 401 J=KK,NGENI
      K=J-NGEN
      YNMF(I,K)=YR(I,J)
401    CONTINUE
402    CONTINUE
      LL=NGEN+1
      DO 405 I=LL,NGENI
      DO 404 J=LL,NGENI
      K=I-NGEN
      L=J-NGEN
      YMMF(K,L)=YR(I,J)
404    CONTINUE
405    CONTINUE
C    OBTAIN THE INVERSE MATRIX FOR YMMF
      CALL DECOMP(NI,YMMF,LI,NI)
      DO 410 I=1,NI
      DRP(I)=CMPLX(0.0,0.0)
410    CONTINUE
      DO 415 I=1,NI
      DRP(I)=CMPLX(1.0,0.0)
      CALL SOLVE(NI,YMMF,LI,NI,DRP,DAVT)
      DO 420 J=1,NI
      BBF(J,I)=DAVT(J)
420    CONTINUE
      DRP(I)=CMPLX(0.0,0.0)

```

```

415     CONTINUE
C   START FORMING THE PRODUCT YNMF*BBF
      DO 430 I=1,NGEN
      DO 425 J=1,NI
      YNMF(I,J)=CMPLX(0.0,0.0)
425     CONTINUE
430     CONTINUE
      DO 440 I=1,NGEN
      DO 435 J=1,NI
      K=1
      L=1
445     YNMF(I,J)=YNMF(I,J)+YNMF(I,K)*BBF(L,J)
      K=K+1
      L=L+1
      IF(K.LE.NI)GO TO 445
435     CONTINUE
440     CONTINUE
      DO 450 I=1,NI
      J=I+NGEN
      JJ=GBUS(J)
      CI(I)=CI(JJ)
      CII(I)=CII(JJ)
450     CONTINUE
      DO 455 I=1,NGEN
      CIF(I)=CMPLX(0.0,0.0)
455     CONTINUE
      IF(KCOUNT.LT.1)GO TO 193
      DO 192 I=1,NI
      CI(I)=CII(I)
192     CONTINUE
193     DO 470 I=1,NGEN
      K=1
      L=1
460     CIF(I)=CIF(I)+YNMF(I,K)*CI(L)
      K=K+1
      L=L+1
      IF(K.LE.NI)GO TO 460
      FK(I)=CABS(CIF(I))
      IF(FK(I).EQ.0.0) GO TO 462
      CIFR=REAL(CIF(I))
      CIFI=AIMAG(CIF(I))
      ALPHAF(I)=ATAN2(CIFI,CIFR)
      GO TO 470
462     ALPHAF(I)=0.0
470     CONTINUE
C   FK'S & ALPHAF'S ARE PARAMETERS OF THE SWING EQUATIONS.
      DO 485 K=1,NI
      L=NI+NGEN+1-K
      M=L
      LLL=L-1

```

```

      DO 480 I=1,LLL
      DO 475 J=1,LLL
      YR(I,J)=YR(I,J)-(YR(L,J)*YR(I,M)/YR(L,M))
475  CONTINUE
480  CONTINUE
485  CONTINUE
      IF(NI.NE.0.0)GO TO 599
      DO 599 I=1,NGEN
      FK(I)=0.0
      ALPHAF(I)=0.0
599  CONTINUE
      KCOUNT=KCOUNT+1
      IF(KCOUNT.GT.1)GO TO 1941
      DO 1937 I=1,NGEN
      DO 1937 J=1,NGEN
      Y1(I,J)=YR(I,J)
      WRITE(10) Y1(I,J)
1937 CONTINUE
      DO 1945 I=1,NGEN
      WRITE(10) FK(I),ALPHAF(I)
      WRITE(6,1930)FK(I),ALPHAF(I)
1930 FORMAT(2F10.6)
1945 CONTINUE
      REWIND 11
      DO 1940 I=1,NBUS
      DO 1940 J=1,NBUS
      READ(11) Y(I,J)
1940 CONTINUE
      READ(15,2000)NFAULT,JFAULT,YF
      IF(NFAULT.EQ.0.AND.JFAULT.EQ.0)GO TO 39
      READ(15,1003)I,J,ZIJ,B
      YF=(1.0,0.0)/ZIJ
      Y(NFAULT,JFAULT)=Y(NFAULT,JFAULT)+YF
      Y(JFAULT,NFAULT)=Y(NFAULT,JFAULT)
      Y(NFAULT,NFAULT)=Y(NFAULT,NFAULT)-YF-CMPLX(0.0,B/2.0)
      Y(JFAULT,JFAULT)=Y(JFAULT,JFAULT)-YF-CMPLX(0.0,B/2.0)
      GO TO 39
1941 DO 1938 I=1,NGEN
      DO 1938 J=1,NGEN
      Y2(I,J)=YR(I,J)
      WRITE(12) Y2(I,J)
1938 CONTINUE
      DO 1950 I=1,NGEN
      WRITE(12) FK(I),ALPHAF(I)
      WRITE(6,1960)FK(I),ALPHAF(I)
1960 FORMAT(2F10.6)
1950 CONTINUE
      STOP
      END

```

C-----



## C        SUBROUTINE DECOMPOSE

```

C-----
SUBROUTINE DECOMP(N,JACOB,LI,N3)
DIMENSION JACOB(90,90),LI(90),JM(90)
COMPLEX JACOB,T
LI(N)=1
DO 6 K=1,N
  IF(K.EQ.N) GO TO 5
  KP1=K+1
  M=K
  LI(K)=M
  IF(M.NE.K)LI(N)=-LI(N)
  T=JACOB(M,K)
  JACOB(M,K)=JACOB(K,K)
  JACOB(K,K)=T
  TM=CABS(T)
  IF(TM.EQ.0.0)GO TO 5
  DO 2 J=KP1,N
2   JACOB(J,K)=-JACOB(J,K)/T
  DO 4 J=KP1,N
  T=JACOB(M,J)
  JACOB(M,J)=JACOB(K,J)
  JACOB(K,J)=T
  TM=CABS(T)
  IF(TM.EQ.0.0)GO TO 4
  DO 3 I=KP1,N
3   JACOB(I,J)=JACOB(I,J)+JACOB(I,K)*T
4   CONTINUE
5   JM(K)=CABS(JACOB(K,K))
  IF(JM(K).EQ.0.0)LI(N)=0
6   CONTINUE
  RETURN
END

```

C-----  
C        SUBROUTINE SOLVE  
C-----

```

SUBROUTINE SOLVE(N,JACOB,LI,N3,DRP,DAVT)
COMPLEX JACOB,DAVT,DRP,D,BV,T
DIMENSION JACOB(90,90),LI(90),DRP(90),DAVT(90),P(90),BI(90)
DIMENSION XM(90),CHP(90,90)
DO 5 I=1,N
  DAVT(I)=DRP(I)
5  CONTINUE
  IF(N.EQ.1)GO TO 9
  NM1=N-1
  DO 7 K=1,NM1
  KP1=K+1
  M=LI(K)
  T=DAVT(M)
  DAVT(M)=DAVT(K)

```

```

      DAVT(K)=T
      DO 7 I=KP1,N
7     DAVT(I)=DAVT(I)+JACOB(I,K)*T
      DO 8 KB=1,NM1
      KM1=N-KB
      K=KM1+1
      DAVT(K)=DAVT(K)/JACOB(K,K)
      T=-DAVT(K)
      DO 8 I=1,KM1
8     DAVT(I)=DAVT(I)+JACOB(I,K)*T
9     DAVT(1)=DAVT(1)/JACOB(1,1)
      RETURN
      END
C  THIS PROGRAM READS IN THE OUTPUT OF PROGRAM 'YBUS'
C  FORMS THE SWING EQUATIONS AND INTEGRATES THE SWING
C26EQUATIONS USING THE SUBROUTINE 'DVERK' FROM THE
C  IMSL LIBRARY.IT CALCULATES INDIVIDUAL MACHINE ENERGY
C  AT EACH TIME STEP USING TRAPEZOIDAL INTEGRATION RULE.
C-----
      COMPLEX YM(40,40),Y1(40,40),Y2(40,40)
      REAL EF(40),HI(40),DEL(40),OMGA(40),PM(40),H(40)
      REAL CF(40,40),DF(40,40),CPF(40,40),DPF(40,40)
      REAL HM(40),Y(80),VP(40),THETA(40),P(40),SEP(40)
      REAL FUNCP(40),FUNCO(40),VK(40),VTOT(40),ANG(40)
      REAL PEE(40)
      REAL C(24),W(80,9),X,TOL,XEND
      EXTERNAL FCN1
      COMMON YM,PM,HI,EF,NGEN
      COMMON FK(40),ALPHA(40),PFK(40),ALPHPF(40)
C-----
C  START READING DATA
      READ(17,1000) NGEN,TSTEP,TCL,TF
1000  FORMAT(I5,5X,3F10.4)
      DO 100 I=1,NGEN
      READ(17,1001)H(I)
1001  FORMAT(F10.6)
100   CONTINUE
      DO 101 I=1,NGEN
      READ(16)KKI,EF(I),DEL(I),PM(I)
101   CONTINUE
      DO 102 I=1,NGEN
      DO 102 J=1,NGEN
      READ(10) Y1(I,J)
102   CONTINUE
      DO 50 I=1,NGEN
      READ(10)FK(I),ALPHA(I)
      WRITE(6,420)FK(I),ALPHA(I)
420   FORMAT(2F12.6)
50    CONTINUE
      DO 103 I=1,NGEN

```

```

DO 103 J=1,NGEN
READ(12) Y2(I,J)
103 CONTINUE
DO 51 I=1,NGEN
READ(12) PFK(I),ALPHPF(I)
WRITE(6,430) PFK(I),ALPHPF(I)
430 FORMAT(2F12.6)
51 CONTINUE
DO 104 I=1,NGEN
DO 104 J=1,NGEN
YM(I,J)=(0.0,0.0)
104 CONTINUE
DO 105 I=1,NGEN
DO 105 J=1,NGEN
YM(I,J)=Y1(I,J)
105 CONTINUE
DO 106 I=1,NGEN
DO 106 J=1,NGEN
CF(I,J)=EF(I)*EF(J)*AIMAG(YM(I,J))
DF(I,J)=EF(I)*EF(J)*REAL(YM(I,J))
CPF(I,J)=EF(I)*EF(J)*AIMAG(Y2(I,J))
DPF(I,J)=EF(I)*EF(J)*REAL(Y2(I,J))
106 CONTINUE
PI=3.14159
DO 107 I=1,NGEN
READ(17,1754) SEP(I)
1754 FORMAT(F8.4)
SEP(I)=SEP(I)*PI/180.
107 CONTINUE
HMT=0.0
DO 108 I=1,NGEN
HM(I)=H(I)/(PI*60.0)
HI(I)=2.0*H(I)
HMT=HMT+HM(I)
108 CONTINUE
DO 109 I=1,NGEN
J=I+NGEN
Y(I)=1.0
Y(J)=DEL(I)
VP(I)=0.0
FUNCO(I)=0.0
109 CONTINUE
C
NW=2*NGEN
N=2*NGEN
TOL=0.0001
IND=1
X=0.0
XEND=0.0
TIMES=0.0

```

```

      IF(TIMES.EQ.0.0) GO TO 110
999    XEND=XEND+TSTEP
99     CALL DVERK(N,FCN1,X,Y,XEND,TOL,IND,C,NW,W,IER)
110    COIA=0.0
      COIS=0.0
      DO 111 I=1,NGEN
        J=I+NGEN
        COIS=COIS+HM(I)*Y(I)*377.0
        COIA=COIA+HM(I)*Y(J)
111    CONTINUE
      COIS=COIS/HMT
      COIA=COIA/HMT
      DO 112 I=1,NGEN
        J=I+NGEN
        OMGA(I)=Y(I)*377.0-COIS
        THETA(I)=Y(J)-COIA
112    CONTINUE
      PT=0.0
C     COMPUTE PCOI
      DO 113 I=1,NGEN
        P(I)=PM(I)-DPF(I,I)
        PT=PT+P(I)
113    CONTINUE
C     CALCULATE INDIVIDUAL MACHINE POTENTIAL ENERGY
      DE=0.0
      NGENN=NGEN-1
      DO 115 I=1,NGENN
        K=I+1
        DO 114 J=K,NGEN
          DE=DE+2.*DPF(I,J)*(COS(THETA(I)-THETA(J)))
114    CONTINUE
115    CONTINUE
      DC=0.0
      DO 301 I=1,NGEN
        DC=DC+EF(I)*PFK(I)*(COS(THETA(I)-ALPHPF(I)))
301    CONTINUE
      PCOIF=PT-DE+DC
      DO 117 I=1,NGEN
        K=I+1
        P(I)=PM(I)-DPF(I,I)
        PEE(I)=0.0
        DO 116 J=1,NGEN
          IF(J.EQ.I)GO TO 116
          PEE(I)=PEE(I)+CPF(I,J)*SIN(Y(NGEN+I)-Y(NGEN+J))+
2          DPF(I,J)*COS(Y(NGEN+I)-Y(NGEN+J))
116    CONTINUE
        PEE(I)=PEE(I)-PFK(I)*EF(I)*COS(THETA(I)-ALPHPF(I))
117    CONTINUE
      DO 118 I=1,NGEN
        FUNCP(I)=P(I)-PEE(I)-(HM(I)*PCOIF/HMT)

```

```

118    CONTINUE
      DO 119 I=1,NGEN
        VP(I)=VP(I)-0.5*(FUNCP(I)+FUNCO(I))*(THETA(I)-SEP(I))
119    CONTINUE
C     COMPUTE THE KINETIC ENERGY
      DO 120 I=1,NGEN
        VK(I)=0.5*HM(I)*OMGA(I)*OMGA(I)
        VTOT(I)=VP(I)+VK(I)
        SEP(I)=THETA(I)
        FUNCO(I)=FUNCP(I)
120    CONTINUE
      DO 121 I=1,NGEN
        J=I+NGEN
        ANG(I)=Y(J)*(180.0/PI)
121    CONTINUE
C     OUTPUT THE RESULTS
      WRITE(20,1061)XEND
1061    FORMAT(/F10.6)
      WRITE(20,1058)
1058    FORMAT(/5X,'COIA',8X,'COIS')
      WRITE(20,1059)COIA,COIS
1059    FORMAT(F9.5,3X,F9.5)
      WRITE(20,1063)
1063    FORMAT(/2X,'GEN#',5X,'OMEGA',8X,'THETA',12X,
1      'POT.EN',11X,'KIN.EN',10X,'TOT.EN',10X,'DELTA')
      DO 1050 I=1,NGEN
        TET=THETA(I)*180.0/PI
        WRITE(20,1062)I,OMGA(I),TET,VP(I),VK(I),VTOT(I),ANG(I)
1062    FORMAT(2X,I3,2X,F8.5,3X,F13.6,3X,F14.8,3X,F14.8,3X,F14.8,
1      6X,F9.5)
1050    CONTINUE
        TIMES=TIMES+1.0
        IF(TIMES.EQ.1.0)GO TO 999
        IF(XEND.LT.TCL)GO TO 9999
        DO 122 I=1,NGEN
          DO 122 J=1,NGEN
            YM(I,J)=Y2(I,J)
            FK(I)=PFK(I)
            ALPHAF(I)=ALPHPF(I)
122        CONTINUE
9999    XEND=XEND+TSTEP
        IF(XEND.LE.TF)GO TO 99
123    CONTINUE
      STOP
      END
      SUBROUTINE FCN1(N,X,Y,YPRIME)
      INTEGER N
      REAL Y(N),YPRIME(N),X
      REAL PE(40),PR(40),EF(40),AP(40)
      REAL C(40,40),D(40,40),PM(40),HI(40)

```

```

COMPLEX YM(40,40)
COMMON YM,PM,HI,EF,NGEN
COMMON FK(40),ALPHAF(40),PFK(40),ALPHPF(40)
DO 10 I=1,NGEN
DO 10 J=1,NGEN
C(I,J)=EF(I)*EF(J)*AIMAG(YM(I,J))
D(I,J)=EF(I)*EF(J)*REAL(YM(I,J))
10 CONTINUE
DO 20 I=1,NGEN
K=I+NGEN
PR(I)=PM(I)-D(I,I)
PE(I)=0.0
DO 15 J=1,NGEN
IF(J.EQ.I) GO TO 15
PE(I)=PE(I)+C(I,J)*SIN(Y(NGEN+I)-Y(NGEN+J))+
1 D(I,J)*COS(Y(NGEN+I)-Y(NGEN+J))
15 CONTINUE
PE(I)=PE(I)-FK(I)*EF(I)*COS(Y(NGEN+I)-ALPHAF(I))
AP(I)=PR(I)-PE(I)
YPRIME(I)=AP(I)/HI(I)
YPRIME(K)=377.0*(Y(I)-1.0)
20 CONTINUE
RETURN
END

```